İZMİR KATİP ÇELEBİ UNIVERSITY

GRADUATE SCHOOL OF SCIENCE AND ENGINEERING

TATTOO DYE REMOVAL USING COLD ATHMOSPHERIC PLASMA (CAP)

M.Sc. THESIS

ELİF ÇUKUR

Department of Biomedical Technologies

Biomedical Technologies Programme

JANUARY 2019

İZMİR KATİP ÇELEBİ UNIVERSITY

GRADUATE SCHOOL OF SCIENCE AND ENGINEERING

TATTOO DYE REMOVAL USING COLD ATHMOSPHERIC PLASMA (CAP)

M.Sc. THESIS

ELİF ÇUKUR
Y160204004

Department of Biomedical Technologies
Biomedical Technologies Programme

Thesis Advisor: Asst. Prof. Dr. Utku Kürşat ERCAN

JANUARY 2019

İZMİR KATİP ÇELEBİ ÜNİVERSİTESİ

FEN BİLİMLERİ ENSTİTÜSÜ

SOĞUK ATMOSFERİK PLAZMA (SAP) KULLANARAK DÖVME BOYASI SİLME

YÜKSEK LİSANS TEZİ

ELİF ÇUKUR
Y160204004

Biyomedikal Teknolojileri Anabilim Dalı
Biyomedikal Teknolojileri Programı

Tez Danışmanı: Dr. Öğr. Üyesi Utku Kürşat ERCAN

OCAK 2019

Elif ÇUKUR, a **M.Sc.** student of **IKCU Graduate School Of Natural And Applied Sciences**, student ID **Y160204004**, successfully defended the thesis entitled "**TATTOO DYE REMOVAL USING COLD ATHMOSPHERIC PLASMA (CAP)**", which she prepared after fulfilling the requirements specified in the associated legislations, before the jury whose signatures are below.

Thesis Advisor :	**Asst. Prof. Dr. Utku Kürşat ERCAN** İzmir Katip Çelebi University	.....
Jury Members :	**Prof. Dr. Murat ELİBOL** Ege University	.....
	Prof. Dr. Aydın AKAN İzmir Katip Çelebi University	.....

Date of Submission : 14 January 2019

Date of Defense : 23 January 2019

To my lovely family,

FOREWORD

First of all, I would like to thank my honorable advisor, Asst. Prof. Dr.Utku Kürşat ERCAN, for determining this thesis topic and for helping me and enlightened me at this thesis studies. He never embarrassed me by not mentioning this situation in spite of the fact that I broke the plasma device countless times or make it inoperative. He was very helpful and consoled to me when I turned the events in my head too much and I was desperate. Thanks to my advisor, dear department academicians and colleagues in a friendly and efficient work environment, I completed all my studies.

I would like to thank all academicians in the Department of Biomedical Engineering and the Department of Biomedical Technologies, especially our dean and our head of the department, Prof. Dr. Aydın AKAN. I would like to thank them, me and all my master student and research assistant colleagues for being friendly, supporting and sharing their valuable knowledge with us.

I would like to thank Prof. Dr. Murat ELİBOL for his valuable time and gave me the opportunity to read my thesis. I hope you like and share your criticism with me.

We would like to thank to the Scientific Research Project council of our university for their value in funding this thesis.

It was very nice to come to school every day thanks to my esteemed master, bachelor, research assistant and lecturer friends you provided me with the family environment and the sincere cooperation. I hope it goes on for years together with every person arrived and departed.

I would like to thank my dear family for their love for me, their support, their soft criticism and the happiness of being together at all times. Even though I was the first child, I think they did a great job in raising me.

I would like to thank my teachers, my family and my friends for helping me to come today and write this thesis.

January 2019 Elif ÇUKUR

TABLE OF CONTENTS

Page

ABBREVIATIONS

CAP : Cold Atmospheric Plasma

BC : Before Christ

AD : anno Domini

Nd:YAG : Neodymium Yttrium Aluminum Garnet

DBD : Dielectric Barrier Discharge

RF : Radio Frequency

UV : Ultraviolet

RS : Reactive Species

ROS : Reactive oxygen species

RNS : Reactive nitrogen species

RONS : Reactive oxygen and nitrogen species

DNA : Deoxyribonucleic Acid

CIE : Commission Internationale d'Eclairage

RGB : Red, Green, Blue

DC : Direct Current

AC : Alternate Current

LED : Light Emitting Diode

PT-DIW : Plasma Treated Deionized Water

LIST OF FIGURES

Page

TATTOO DYE REMOVAL USING COLD ATHMOSPHERIC PLASMA (CAP)

ABSTRACT

Tattoo has been used as a method of self-expression of mankind since ancient times. The tattoo removal process with primitive methods is based on the process of peeling the skin layer on which the tattoo is placed. Besides being used today, laser is preferred by more people. The tattoo removal with laser is based on disintegration into smaller pieces by breaking the target tattoo pigment by absorbing the transmitted beam. It is then transferred to the nearest lymph node or disintegrated by the macrophages by means of blood or lymph circulation. The most common difficulty with laser tattoo removal application is that the laser wavelength is designed to ensure that the wavelength is not matched with the melanin pigment in red, yellow and green colors close to the skin color. In addition, tattoo dyes containing iron and titanium (mostly red and black tattoo paints), instead of absorbing most of the laser beam onto it, reflects both darkening of the tattoo dye and thermal side effects in the surrounding tissue. Except in these special cases, laser tattoo removal can cause skin rashes, hyperpigmentation, hypopigmentation, itching, allergic reactions, wound formation and bleeding.

Considering the disadvantages of laser tattoo removal, and tooth whitening effect of cold atmospheric plasma treatment for tattoo dye degradation was investigated on six different color tattoo dyes. The fourth state of matter, plasma, in this study in cold form and ambient air conditions used as color fading effect on tattoo dyes. The aim of this study is to investigate the direct and indirect efficiency on tattoo dye by reactive species and ultraviolet radiation during the formation of plasma. In the light of the results, treatment of the cold atmospheric plasma both directly and indirectly to the tattoo dye has been accomplished color degradation in all colors. Plasma, which was advantageous compared to laser applications by providing color fading especially in red, yellow and green colors, showed a parallel behavior with the color fading on black tattoo dye.

SOĞUK ATMOSFERİK PLAZMA (SAP) KULLANARAK DÖVME BOYASI SİLME

ÖZET

Dövme antik çağlardan beri insanoğlunun kendini ifade etme yöntemi olarak kullanılmıştır.
İlkel metotlar ile dövme silme işlemi, dövmenin yerleştirildiği deri katmanının soyulması işlemine dayanmaktadır. Günümüzde hala kullanılmalarının yanı sıra lazer daha fazla kişi tarafından tercih edilmektedir. Lazer ile dövme silme işlemi, hedef olan dövme pigmentinin gönderilen ışını absorbe etmesi ile parçalanıp daha küçük parçalara ayrılır. Daha sonra kan veya lenf dolaşımı yardımı ile en yakın lenf noduna aktarılır veya makrofajlar tarafından parçalanır. Lazer ile dövme silme işlemlerinde en çok karşılaşılan zorluk, lazer dalga boyunun melanin pigmenti ile eşleşmemesini sağlayacak şekilde tasarlanmasından dolayı deri rengine yakın kırmızı, sarı ve yeşil renklerde görülmektedir. Ayrıca demir ve titanyum içerikli, üzerine gelen lazer ışınının çoğunu absorbe etmek yerine yansıtan dövme boyası pigmentleri (daha çok kırmızı ve siyah renkli dövme boyaları) hem dövme renginin koyulaşmasına hem de çevre dokuda termal yan etkilere sebep olmaktadır. Bu özel durumlar haricinde lazer ile dövme silme işlemi deride kızarıklıklara, deri renginin koyulaşmasına veya açılmasına, kaşıntı ve alerjik reaksiyonlara, yara oluşumuna ve kanamalara sebep olabilmektedir.
Lazerin dezavantajlarından ve soğuk atmosferik plazmanın diş hekimliği uygulamalarından yola çıkarak bu çalışmada, dövme boyası degradasyonu için soğuk atmosferik plazma uygulaması altı farklı renk dövme boyası üzerinde araştırılmıştır. Maddenin dördüncü hali olan plazma, bu çalışmada soğuk formda ve ortam gazı olarak hava kullanılarak dövme boyası üzerinde renk açıcı özellik göstermiştir. Bu araştırmanın amacı soğuk atmosferik plazmanın oluşumu sırasında ortaya çıkan reaktif türler ve ultraviyole ışınlar sayesinde dövme boyası üzerindeki doğrudan ve dolaylı etkinliği araştırılarak lazer uygulamalarına yardımcı veya alternatif bir dövme silme metodu ortaya koymaktır. Elde edilen sonuçlar ışığında, soğuk atmosferik plazmanın hem doğrudan hem de dolaylı olarak dövme boyasına uygulanması sonucunda tüm renklerde açılma gözlemlenmiştir. Özellikle kırmızı, sarı ve yeşil renklerde renk açılması sağlayarak lazer uygulamalarına göre avantaj sağlamış olan plazma, siyah dövme boyasındaki renk açılması ile lazere paralel bir davranış göstermiştir.

1. INTRODUCTION

1.1. Tattoo

Tattoos have been fascinated human being from all cultures and degrees of society for centuries and the aim of tattoo designs varies from culture to culture and its place on the time line. The word tattoo is derived from the word “ta-tu” in the Tahitian language which meaning "to strike" [1].

According to the historical records, the oldest tattoos were found in the Egyptian civilization and as the Egyptians expanded their boundaries, the tattooed people increased proportionally [2]. After Egypt, tattoo art was adopted by Greek, Persian and Arabian civilizations. About BC In 2000, a spread of tattoo from Egypt to China has been seen. In Greek society, the tattoo was designed in a variety of ways to get to know each other by government officials who were in a secret position. While in Romans used criminals and slaves to separate them from the rest of society. In early Britain societies, the tattoo became an important place for the noble class and was widely used in the family armaments until it was banned by the pope in 787 AD [3].

In ancient times; various bones, rock fragments and wood tools were used to transfer tattoo pigments to the skin. While the tattoo pigments were obtained from natural materials such as various plants, flowers, juices or dried tree barks [4]. By 1891, tattooing became more common in the society with the invention of the first electric tattooing device. Tattooing with the invention of electric tattoo device has become a common pleasure to be achieved for plenty of people. With such a spreading of the tattoo, unfortunately, in cases where adequate hygiene conditions are not provided, hepatitis, blood poisoning and other diseases caused by tattoos have been observed. Especially in 1961, these diseases were the most common [5]. By the 21st century, the demand for tattooing has been increased and the popularity has reached which has never been shown before.

The tattoo tools have a 2000-year history according to known sources. The first tattoo tools are made of a durable wood or mine with a pointed tip and a hole in the

center that contains pigments to be used for tattooing. Nowadays, the creation mechanism of permanent tattoo can be defined as puncturing the skin with needles to mechanically deliver ink, which contains tiny fragments of pigments situated in a carrier, into the dermis of an individual [6].

Current electric tattooing equipment consists of 3-5 small tattoo needles which are very small and thin needles that are arranged in a row in the electric tattoo device and moving synchronously. Whereby the fast vibrating movement of needles, pigment-containing ink is transferred from the epidermis and down to the dermis as shown on figure 1.1. In principle, permanent tattooing, ink containing insoluble and non-biodegradable colorants is the process of mechanically opening holes in the upper surface of the epidermis by the needles and placing them in the dermis layer [6].

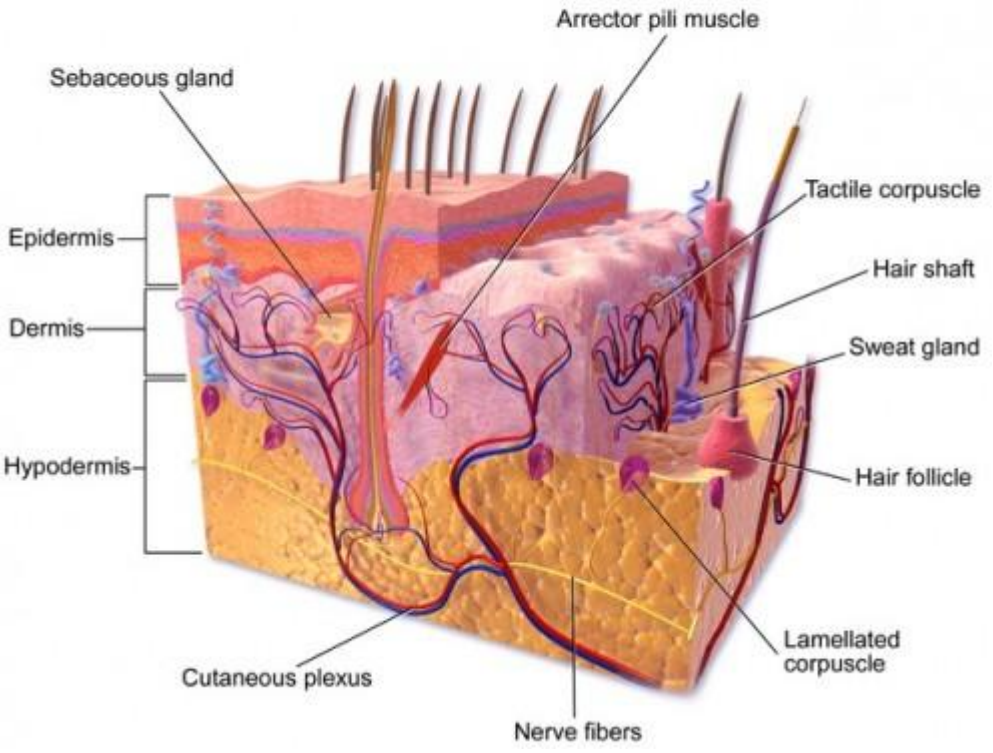

Figure 1.1 : Structure of human skin.

The so-called basement membrane found in the epidermis inhibits the passage of the tattoo pigment from the epidermis and the punctures created by the needles can only allow 1/3 of the tattoo to remain in the dermis [6].

42 days after the tattoo, the tattoo pigment that was left in the epidermis and dermis initially decreased to 32% of the amount of pigment transferred. In the so-called initial phase, weeks after the tattoo is made, tattoo ink starts to migrate from where it was first placed or to create other compounds similar to the chemical composition own itself first times [6].

During the healing process, 70-80% the ink particles are eradicated by fibroblasts and macrophages or are held on to the extracellular matrix of dermis and the remaining ink particles are found such that 10-15% of the ink particles lie flattened on collagen fibers and 5-10% of the ink particles lie attached on the serosal side of capillaries [7]. That is, approximately one third of the first injected tattoo paint remains in the skin as permanent tattoo.

The chemical components of permanent forging tattoo products vary widely according to the color of the pigment and the manufacturer. In this study, since six color tattoo dyes are selected to examine the degradation of tattoo dyes, the chemical compounds seen in these tattoo dyes are summarized. Black color of permanent tattoo dyes consist of generally iron oxide and carbon and also they are quite rarely bring about allergic circumstances. Red color of tattoo dyes involves mercuric sulfide (cinnabar), cadmium red and iron oxide compounds usually. Cinnabar and cadmium pigments are poisoned. Cadmium yellow and ochres uses for create yellow color tattoo dye. Yellow pigments seldomly occasion allergic circumstances. Chromic oxide, lead chromate and phthalocyanine dyes utilizes for green color pigments. Blue colored tattoo dyes contain cobalt, copper phthalocyanine and cobalt aluminate. In pigments that give a green and light blue color, allergies are often associated with chromium, aluminum or chloride cobalt compounds. White color of tattoo dyes instore them inside lead carbonate titanium dioxide and zinc oxide. Titanium oxide is white color tattoo pigment that shows minimum allergic response but, it reflects most of the beam sent when laser tattoo removal method is used [8].

1.2. Tattoo Removal Methods and Disadvantageous of Lasers

The person with the tattoo may decide on the tattoo removal process for the tattoo to lose its meaning, blur, or for other reasons. Over the years, many different tattoo removal methods have been investigated. Until the methods of laser tattoo removal, the old methods were based on mechanical, chemical and thermal processes which

arised from peeling the epidermis. Such as, dermabrasion is a skin regeneration method by sanding the skin's outer layers [9]. And the other mechanical method, salabrasion uses table salt for peeling the outer skin layer [10]. Cryosurgery is the method in which liquid nitrogen is used to pare the epidermis [11]. And the thermal method, the stripping of the surface of the skin to the desired depth with a metal probe at high temperature is carried out in cauterization [12].With the development of technology, the aforementioned painful tattoo removal methods were replaced by laser treatment. Permanent tattoo removal method with laser is performed by wavelength applied according to selective photothermolysis [13] principle of laser according to the color, size and the position of tattoo. In that the wavelength makes use of tattoo removal should link with the absorption spectrum of tattoo ink [14]. The tattoo pigments disjunction by the laser are carried by the lymphatic system and tattoo color begins to appear lighter. Determination of the most appropriate laser wavelength for the tattoo to be removed is committed according to the absorption and reflection characteristics of the pigment or pigments [15]. The laser wavelength should be selected so that the color of the targeted tattoo dye as well as keeping absorption at minimal level by primary endogenous chromophores, hemoglobin, and melanin. In order to avoid damaging the skin with the laser, the pulse duration should be kept briefer than the thermal relaxation time and brief pulses should be utilized at the nanosecond level. [16]. Multicolor tattoos, molecules that should not be targeted and nanosecond pulses require the use of highly demanding tattoo removal processes.

Nowadays, the lasers used for tattoo removal are generally matched by the color of the tattoo to be faded and the wavelength of the laser to be used. The oftenest employed wavelengths are; 510 nm (pulsed-dye laser) for degrading yellow inks, 1064 and 532 nm (Nd:YAG laser) for degrading black and red inks respectively, 694 nm (ruby laser) for degrading blue, black, and green inks, and 755 nm (alexandrite laser), for degrading blue and black inks [9]. Due to monochromatic structure of the lasers, the laser type should be selected according to the color of targeted tattoo dye. For this reason, multicolor tattoos require multiple laser types to be preferred during the removal process or more sessions are required. This causes the enlarged time for the tattoo removal process to increase and the cost to increase [17].

Like multicolor tattoos, laser-based tattoo removal methods have additional shortcomings. For example, lasers induce heating of the skin and can cause burns, undesirable tissue damage, scarring or color variations that are likely to remain after healing. Current laser-based procedures could be somewhat ineffective at complete removal of tattoo inks, require multiple treatments at a high cost, cause pain, and can result in scarring, disfigurement, and depigmentation of the treated skin [17].

A variety of deformations could occur on the skin surface as a result of applying the tattoo removal with laser (Figure 1.2). In the epidermis, superficial whitening of the skin can be seen in which melanocytes, due to the absorption of energy by melanin, cause the balloon and become hyperchromatic. The most common side effects with Q-switched ruby laser include textural changes, scarring and pigmentary changes. The reason why hypopigmentation, which often observed temporarily, have seen is the absorbance of the laser which is spreading at 694 nm wavelength by the melanin pigment [18]. Fitzpatrick *et al.* emphasized that Q-switched alexandrite laser, transient hypopigmentation in as much as 50% of patients and a 12% incidence of textural changes has been reported [19]. In other cases, reduced melanin pigmentation and brown shells were observed in a manner similar to a worn wound [20]. The pain associated with the balloons formed in the epidermis and dermis layer was found to be more severe in dark-skinned individuals and in tattoos containing dense tattoo pigment [21]. Whitening and graying of the skin after application, small size bleeding in some areas, inflammation and tissue splattering in some patients were observed. Large-scale bleedings, tissue scattering and inflammation were beheld after administration at high doses [22].

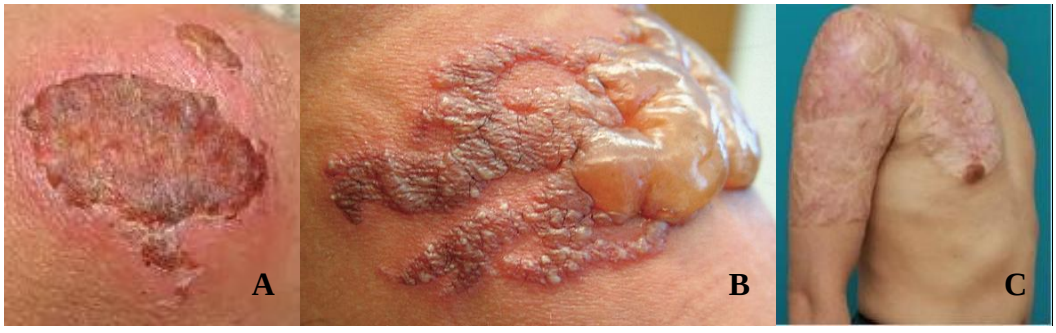

Figure 1.2 : A: Brown shells (A), inflammation (B), and whitening (C) images on the skin as a result of tattoo removal applications with laser.

Aim of the present study was to analyze possible effects of non-thermal atmospheric DBD air plasma on degradation of tattoo inks *in vitro* for possible future utilization

of cold plasma technology in clinical tattoo removal procedures either by itself or as an assistive method to laser.

1.3. Cold Atmospheric Plasma

Irving Langmuir named after 'plasma' by inspiring the non-cellular part of blood which can be defined as the fourth state of matter, this is also described as an ionized gas community [23].

1.3.1. Plasma physics

Plasma was **described** by Sir Crooke in 1879 [24] and was firstly named after by Langmuir in 1929**.** Plasma can be found in various forms and can be built in diversified paths. Plasma is an ionized gas. Ionization is described as a process that an atom or molecule gains or losses of electrons. In consequence of ionization the molecule or atom turns into positive or negative form depending on the gain or loss of electron respectively. When the temperature rises, molecules gains energy, it occurs transform plasma as a fourth state after solid, liquid, gas phases. During generation of plasma, electrons take energy much faster than heavier particles with the effect of electrical field. Electrons and ions cause plasma electrically conducting and responsive [25]. In the entire plasma that is provided by electric field, the electrons take the external energy much quicker than the heavier ions and have the possibility of warming up to thousands of degrees before the surrounding area heats up. In thermal plasma, the energy flow from electrons to heavy particles is balanced when the temperature of the heavy particles is nearly even to the electron temperature. While in non-thermal plasma, the ions and neutral molecules remain cold, which is more effective than the energy transfer from electrons and the gas maintains at low temperature. Therefore non-thermal plasma is named non-equilibrium plasma, as well. Thanks to this feature, non-thermal plasma (because it does not expose to thermal side effects) is widely preferred in medical applications (Figure 1.3) [26].

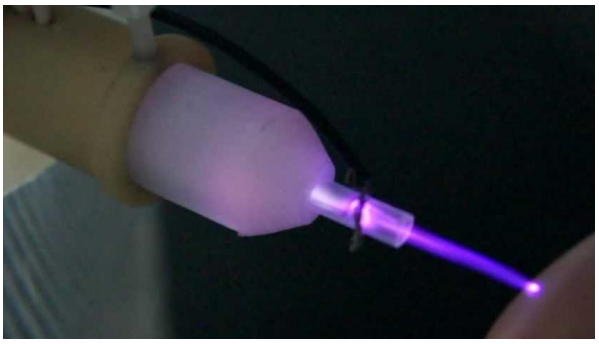

Figure 1.3 : Cold atmospheric plasma in air jet form.

In direct plasma treatment, the plasma discharge is applied directly to the targeted sample. That is, one of the electrodes is living tissue itself, plasma treatment on live tissue. In direct cold plasma treatments where the electric field is formed in high voltage (10–40 kV) and ambient air, the discharge current must be kept at certain limit values in case treatments carried out on living tissue. [26]. In indirect plasma treatment, the plasma discharge is generated in a region that is not in contact with the treated material and the plasma products are carried with a gas flow. In addition to direct and indirect applications, in fluid mediated plasma treatment a fluid is treated with direct plasma, which leads chemical modifications in the fluid, and then the treat fluid is transferred to the target substance. In fluid mediated plasma treatment of fluid is considered as direct and transferring fluid to a substance is considered as indirect plasma treatment [26].

In various studies to date, non-thermal plasmas have been used in various gas mixtures, pressure values and flow rates, and have undergone specific changes in material to be applied with various power supplies and electrode designs. Dielectric barrier discharge (DBD) plasma is a kind of the direct application method used in plasma medicine commonly due to its flexibility. DBD set up consists of one high voltage and one grounding electrode and quite a few DBD devices are employing at high frequencies (Figure 1.4). In design of DBD electrode, at least one of the electrodes could be coated to show dielectric property with an insulating material such as glass, ceramic, quartz. Presence of dielectric material is used to avoid arc formation and limits and it distributes the current over a large area. DBD is largely implemented for ozone product in UV-source [27].

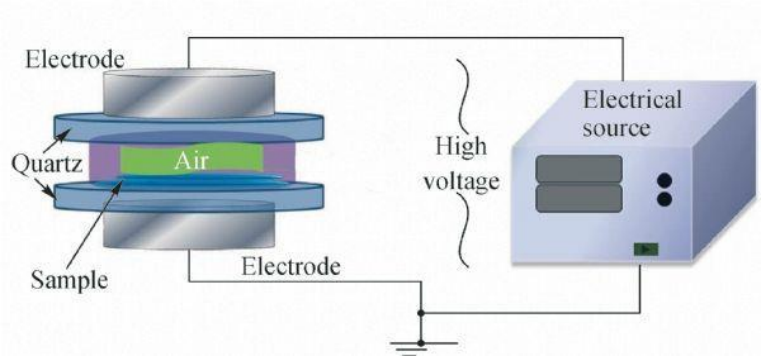

Figure 1.4 : DBD plasma diagram.

1.3.2. Plasma chemistry

Cold atmospheric plasma influences viruses, bacteria and eukaryotic cells through ultra violet (UV) radiation, free radicals and reactive species (RS) generated by the electric field. While the electric field is implemented to gas that is in the environment, electrons are accumulated to get higher energy. These electrons collide with gas atoms and molecules. It causes to generation of positively charged ions because of electron lost from ambient gas. It makes their contribution important in plentiful plasma-chemical process. Moreover, for high chemical activity, atom and molecule ions are able to have substantial kinetic energy that decides their additive in reactions [25].

At cellular level, atmospheric cold atmospheric plasma may exhibit beneficial and detrimental effects due to reactive oxygen species (ROS) and reactive nitrogen species (RNS) relative to the molecules in which the plasma is formed [28]. When began with malignant influences of over-produced reactive oxygen and nitrogen species (RONS) in cellular level, it causes destructive effects including lipids, cell membranes, proteins and DNA that cause oxidative stress. [28]. On the other hand, the beneficial influences of RONS are seen in moderate values. Some of the most preferred areas in the plasma medicine section are given.

It has long been a proven fact that reactive species produced by mammalian immune system cells play an important role in creating resistance to viral and bacterial diseases [29]. At cellular level, reactive species organize cell differentiation, division, migration and apoptosis [30-33]; they check cell-to-cell adhesion [33], biosynthesis of growth factors and collagen production [34]. For example, Sen *et al.* examined of hydrogen peroxide (H_2O_2) at different concentration ranges either stimulates or inhibits cell proliferation or induces cell apoptosis [35].

Reactive species are generated through various collisional pathways, such as electron impact excitation and dissociation. Reactive species play an important role in all plasma–surface interactions. Reactive species produced by excited electrons give rise to excitation and separation reactions by having a significant impact in the interaction of plasma with the surface to which it is applied. A number of reactions that give rise to produce of some species in plasma treated environment:

$$O + O_2 + M \rightarrow O_3 + M$$

$$N + O + N_2 \rightarrow N_2 + NO$$

$$NO + O_3 \leftrightarrow NO_2 + O_2$$

$$NO + O_3 \leftrightarrow NO_2 + O_2$$

$$NO_2 + O_2 + hv \rightarrow O_3 + NO$$

$$H_2O + O_3 \leftrightarrow O_2 + OH^-$$

$$e + H_2O \rightarrow OH + H + e$$

$$O + H_2O \rightarrow 2OH^- \quad (1.1)$$

When the electric field was supplied to an environment to create cold atmospheric plasma, ultraviolet radiation formed with reactive species. The environment in which the electric field is passed affects both the reactive species to be formed and the formation of UV radiation. For example, in experiments with bacterial inactivation with DBD plasma only in an environment with argon gas, bacterial inactivation was observed because of UV luminescence based on noble gas, argon [36]. In contrast with argon gas due to the high chemical activity of oxygen radicals in atmospheric air, it is less efficient in plasma discharge and does not emit UV. [36]. Thus, whether UV is formed or radiation intensity depends on the gases in the electric field generated environment and their chemical activity.

When we look at the cellular effects of UV radiation at the molecular level, it is observed that direct applications cause cellular oxidative stress. Direct effects of UV radiation include modifications of DNA and macromolecules, UV radiation induces the release of intracellular RS, which in turn cause oxidative degradation of lipids and oxidative DNA damage [37].

The interaction of ions and reactive species formed by plasma treatment can change pH of the medium and the sample applied to the plasma. As the electric field applied to water, by dissolving the nitrogen oxides (NO_x), water will become acidified by cold plasma in ambient air [38]. The RONS components (O•, NO•, NO_2, O_3, and OH•) formed as a result of plasma applied to atmospheric air can show the following reactions that cause acid formation and the corresponding pH drop [39]:

$$2NO + H_2O + O_3 \rightarrow 2HNO_3$$

$$NO + O_3 \rightarrow NO_2 + O_2$$

$$NO_2 + OH \bullet \rightarrow HNO_3 \qquad (1.2)$$

In applications of cold atmospheric plasma with water, it has been identified that hydrogen peroxide (H_2O_2) and nitric oxide (NO_x) components are repeated in acidic conditions. Hydrogen peroxide (H_2O_2) and nitrite (NO_2) combined in acidic terms (presence of H^+ or H_3O^+) cause the formation of peroxynitrite and then transform to OH and NO_2:[40]

$$NO^2 + H_2O_2 + H^+ \rightarrow O = NOOH + H_2O$$

$$O = NOOH \leftrightarrow OH + NO_2 \qquad (1.3)$$

Therefore, the bactericidal effect of the cold atmospheric plasma after interaction with water includes at low pH ambient, nitrites and peroxide, toxic effect of chemically active species (NO, NO2, OH and ONOOH) and addition of ozone to the liquid by the effect of plasma [28].

1.3.3. Plasma medicine

Plasma medicine is an area where thermal and mostly non-thermal plasma interactions are widely researched in various fields.

Thermal plasmas can be used for cauterization, tissue removal, cutting tissue, sterilization of medical tools. Also non-thermal plasma treatment employed for protecting resistant microorganism to antibiotics, and hospital infections. In addition to the topics such as wound healing, bleeding controlling, dental treatment, and cancer which have been emphasized recently in plasma medicine, promising issues such as surface modification on biomaterials, creating new drugs are also studying [26].

The antimicrobial activity of the cold atmospheric plasma with oxidative stress is provided by reservoir of charged particles in electrostatic force applied environment. The diffusion of ROS bring about to local harm by oxidation to the cytoplasmic membrane, proteins, DNA material and lysis of bacteria consequently the fragmentation of membrane [41]. Cold atmospheric plasma causes apoptosis and necrosis at cellular level due to reactive species due to ambient gas and presence density. CAP has been used to treat antimicrobial properties as mentioned above, as well as in the treatment of cancer.

RONS are therapeutically active agents in some cases by neoplastic cells by enhancing the density of oxygen and nitrogen species. The formation of reactive species from radiation and inflammation is thought to be connected with carcinogenic cells [42]. CAP studies on cancer cells have shown that low doses of treatments cause apoptosis. It includes of specific structural changes such as cell contraction, core fragmentation and chromosome concentration after plasma treatment. The apoptotic cell fractions are then swallowed and eradicated by phagocytic cells. Thus, it demonstrates the advantage of CAP according to other methods of cancer treatment, with the absence of toxic cellular particles that are frequently seen in the case of necrosis and the absence of inflammatory changes [28].

Prion inactivation, one of the most challenging areas of medical sterilization, is one of the areas where cold atmospheric plasma is applied. Prions, in which traditional sterilization methods have failed, can be defined as a misfolded protein. Prion is so compelling that it is more resistive to outer influences than bacterium, viruses and fungus [43].

1.3.3.1. Plasma disinfection

Disinfection with cold atmospheric plasma has an important place in plasma medicine especially when medical devices and operations are concerned with sterilization of instruments [44]. The process of disinfection with cold atmospheric plasma has been tested in gram-positive, gram-negative bacteria, biofilms, viruses and fungi [45]. These studies show that the effect of plasma on microorganisms differs in two ways. The first is to seriously damage the physical structure of microorganisms and cause sudden cell death. And second, to create holes in the cell membrane that cause less serious damage and to change the physical and chemical structure of the membrane to cause gradual cell death [44].

Plasma sterilization depends on an assembly of factors like ozone, UV photons and reactive species. It is called as oxidative stress in living organisms in case of regression of homeostasis by increasing the number of reactive oxygen species.

Some antimicrobial trials with CAP can be summarized as follows. Deng *et al.* demonstated that in cold atmospheric surface microdischarge plasma applications on *Candida albicans, Bacillus subtilis, Bacillus pumilus, Bacillus atrophaeus* and *Geobacillus stearothermophilus*, indicated the high inactivation rate was independent of the material of the test specimen [45]. Klämpfl *et al.* developed an indirect plasma device in 2005 the Max Planck Institute for Extraterrestrial Physics in Garching, Germany, called MicroPlaSter (built by ADTEC Plasma Technology Co. Ltd., Hiroshima, Japan and London, U.K.). The system was indicated a bacterial load drop of 99.9% on MRSA (Methicillin-resistant *S.aureus*) after 2 minutes plasma treatment. The above examples showed significant results in terms of plasma disinfection and showed that it could inactive microorganisms that cause hospital acquired infections. [46]. As the direct cold plasma applications show antimicrobial activity, the plasma-treated carriers have been shown to exhibit this effect. As with the direct effect of cold atmospheric plasma, indirectly it causes bacterial inactivation by the effect of reactive species and UV radiation. In cases where plasma is imposed indirectly, bacterial inactivation may also lead to various chemical and physical changes due to reactive species and UV in the material where charged particles are expected to produce indirect effects, and are transferred to secondary target materials [48].

Antimicrobial properties of cold atmospheric plasma have been used not only in clinical studies, but also in agriculture since the reactive species formed by the plasma do not cause penetration from the surface of the substance, formal changes are only observed on the surface of the food [48,49].

1.3.3.2. Plasma dentistry

The applications of plasma in dentistry can basically be summarized in two groups [50]. The first of these is to provide the creation of optional, qualified surfaces by utilizing the surface modification properties of the material that plasma is applied to, and also to use the antimicrobial property of plasma. The other is the use of cold atmospheric plasma in the mouth for therapeutic goals. Titanium implants, which are

widely used in dental applications, showed changes in the hydrophilicity of the titanium surface when plasma treatment was performed, and cellular adhesion rate increased due to the change of surface roughness [51,52], besides no residues after treatment. When it comes to plasma treatment of zirconia implants were demonstrated titanium-like effects [53,54]. It was confirmed by various studies that the polymerization after plasma treatment was increased [55] with the dental filler and adhesive polymers used in dentistry and the compounds synthesized by the plasma were successful in terms of high polymerization and binding to the tooth surface [56]. In contrast to the heavy chemicals used in traditional cleaning methods in dentistry, it creates wastes in the non-toxic gas (CO_2, H_2O, and N_2) after plasma application [57,58]. Hydrogen peroxide (H_2O_2) is a prevalent bleaching chemical compound in dentistry and known as effective and safe [59]. Traditional teeth bleaching methods usually utilize a 30%–44% H_2O_2 bleaching gel and a high-intensity light source [60,61]. This source of light used can increase bleaching but unfortunately cause thermal side effects on the tooth surface. In contrast to conventional tooth bleaching methods, it was seen that toxic side products were not produced by plasma-produced reactive species and has successfully provided teeth bleaching as shown at figure 1.5. [62,63].

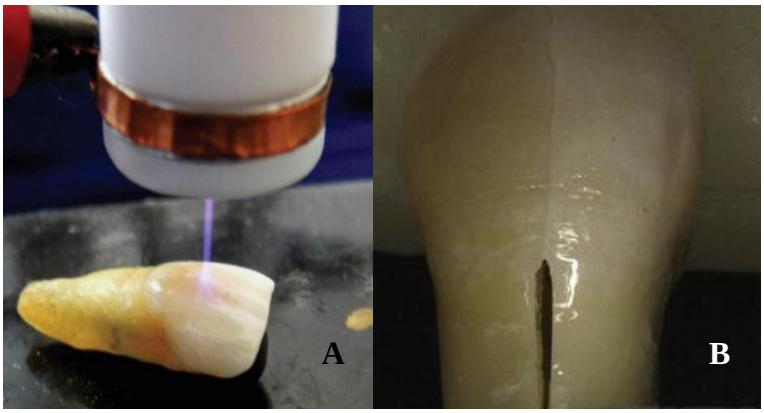

Figure 1.5 : Cold atmospheric air jet plasma application on tooth (A) and before (image B left side) and after (image B right side) the application of cold atmospheric plasma with hydrogen peroxide.

1.3.3.3. Plasma applications in wound healing and dermatology

In addition to dentistry and sterilization, wound healing applications are one of the most studied areas of cold atmospheric plasma.

When a wound is opened, the skin begins to repair and renew itself through regular biochemical work. The wound healing process can be briefly summarized as cellular migration from other parts of the area where cells are separated, localization, proliferation, differentiation and apoptosis. It has been confirmed that the wound inflammatory process is shortened and the proliferation of fibroblasts and other cells is accelerated by the reactive species formed in the plasma applied medium [64].

Besides performing the targeted effect in cold atmospheric plasma applications on the skin surface for antimicrobial activity or wound healing, skin physiology variables containing barrier function, hydration, skin temperature and carotenoid grade were transient affected by plasma treatment. Cold atmospheric plasma treatment is considered safe in terms of skin physiology applications, since plasma does not damage the skin surface and the mechanism of operational structure of skin [65].

Plasma applications in dermatology briefly collected as the treatment of eczemas, dermatitis, ulcerous injuries with local and systemic angiitises, and a couple of other skin diseases [66]. For example, a reduction in *S.aureus* colonization on the skin and a decrease in atopic eczema-induced itching were observed as a result of DBD plasma treatment [67]. Fetykov *et al*. examined an *in vivo* study, and it was found that the time of complete wound healing in diabetic foot disease was halved by using an indirect cold plasma jet system called Plasmafon. In addition, there was a decrease in pain within 5 days after treatment and first re-epithelialization of the borders after 10 days of plasma treatment [68]. In a study conducted with the MicroPlaSter plasma torch, patients which have chronic infected dermal wounds were exposed to cold atmospheric plasma application for 5 minutes daily and there was a high incidence of decrease in plasma-treated bacterial colonization compared to untreated sites [69]. In another study conducted with MicroPlaSter by Isbary *et al.*, individuals with Hailey-Hailey disease were treated with argon plasma cure for 5 minutes and after 4 treatments the skin lesions were healed with relief of the stinging sensations [70]. In one of the cold atmospheric plasma studies involving plasma medicine in dermatology and cancer applications, plasma device using Surface Micro Discharge (SMD) operated in ambient air was applied on melanoma cells. Irreversible melanoma cell inactivation and induction of apoptosis were observed

after 2 minutes of plasma application on malignant melanoma with the miniFlatPlaSter [71].

1.4. Color and Color Spaces

Color perception arises from the stimulation of cone cells in the human eye by electromagnetic radiation in the visible spectrum. The classification of colors and the measuring of wavelengths are realized by comparing the wavelength of the beam reflected from the surface of the object. By defining a color space as internationally accepted by the International Commission on Illumination (CIE) in 1931, the colors can be expressed in numerical terms with specific coordinates [72].

1.4.1. CIE RGB color space

RGB color space is depicted as the three chromaticities, which means quality of a color regardless of its luminance, of the red, green, and blue additive primaries, and can generate any chromaticity that is the triangle identified by those primary colors. For example, the RGB color space is divided into three wavelengths similar to the excitation wavelengths of cone cells in the human retina: long wavelength (564–580 nm) matches with red color, medium wavelength (534–545 nm) matches with green color and short wavelength (420–440 nm) matches with blue color. RGB is a color model suitable for computer graphics because the human visual system operate in a similar way to RGB color space [72,73].

The standardized CIE RGB color matching functions $\bar{r}(\lambda)$, $\bar{g}(\lambda)$, $\bar{b}(\lambda)$ obtained using three monochromatic primaries at standardized wavelengths of 700 nm (red), 546.1 nm (green) and 435.8 nm (blue). For example, $\bar{r}(\lambda)$ and $\bar{g}(\lambda)$ are zero at 435.8 nm, $\bar{r}(\lambda)$ and $\bar{b}(\lambda)$ are zero at 546.1 nm, and $\bar{g}(\lambda)$ and $\bar{b}(\lambda)$ are zero at 700 nm, since in these cases the test color is one of the primaries [72].

The RGB values for a color with a spectral power distribution $\bar{S}(\lambda)$ would then be given by [72]:

$$R = \int_0^\infty S(\lambda)\bar{r}(\lambda)d\lambda$$

$$G = \int_0^\infty S(\lambda)\bar{g}(\lambda)d\lambda$$

$$B = \int_0^{\infty} S(\lambda)\bar{b}(\lambda)d\lambda \quad (1.4)$$

After spectral power distribution operations, the color value in each pixel of the object image that is digitized takes a value between 0 and 255. When each of the RGB values is 0, the color of the pixel is black and white when it is 255. Again, each of the RGB values will have gray tones when they get the same numerical value between 0 and 255. The differentiation of the RGB values between each other causes the image to become reddish, greenish and bluish.

1.4.2. CIE XYZ and CIE Yxy color spaces

The color spaces defined by the CIE in 1931 were the first to describe the connection between the color in the color perception process and the place in the electromagnetic spectrum [74]. Since color of the observed object varies according to the conditions of the environment and the type of light source, the RBG color space will be insufficient when the image needs to be digitally reconstructed. This can be exemplified by the same object photographed in sunlight and in a room illuminated by fluorescence, giving different RGB values in the specified pixels. When the color matching functions between the specific pixels of the objects displayed in two different environments are considered, CIE XYZ color space is more successful than RGB [75].

The CIE XYZ color matching functions $\bar{x}(\lambda)$, $\bar{y}(\lambda)$, and $\bar{z}(\lambda)$ give the relative contributions of light with wavelength λ to the CIE tristimulus values X, Y, and Z. The color matching functions were detected by calculating the mean color perception of a sample of human observers over the visual range from λ_{violet}=380 to λ_{red}=780 nm. To calculate CIE X, Y, and Z values for light with spectrum $P(\lambda)$ we sum, over the visual spectrum, the products of the color matching function weights at each wavelength and the intensity emitted at a constant narrow wavelength interval centered there:

$$X = \Delta\lambda \sum_{\lambda=\lambda_{red}}^{\lambda_{violet}} \overline{x_\lambda}\, P(\lambda)$$

$$Y = \Delta\lambda \sum_{\lambda=\lambda_{red}}^{\lambda_{violet}} \overline{y_\lambda}\, P(\lambda)$$

$$Z = \Delta\lambda \sum_{\lambda=\lambda_{red}}^{\lambda_{violet}} \overline{z_\lambda}\, P(\lambda) \quad (1.5)$$

The X and Z components give the colour or chromaticity of the spectrum. The detected color only depends on the relative magnitudes of X, Y, and Z, we determined its chromaticity coordinates as:

$$x = \frac{X}{(X + Y + Z)}$$

$$y = \frac{Y}{(X + Y + Z)}$$

$$z = \frac{Z}{(X + Y + Z)}$$

$$x + y + z \equiv \frac{X+Y+Z}{X+Y+Z} \equiv 1$$

$$z = 1 - (x + y) \tag{1.6}$$

Thus, chromaticity coordinates are generally given as just *x* and *y* [76]. Each x, y, z data takes a value between 0 and 1, in CIE XYZ color space. The derived color space specified by x, y, and Y is known as the CIE xyY color space and is often employed to indicate colors in practice. While the x and y components give information chromaticity, the Y component contains luminance data. While the chromaticity value changes between 0 and 1, the brightness is between 0 and 100. The value of 0 represents black for each variable (x, y, and Y), while 100 represents white for only brightness (Y value). For the x and y axes, which give the chromaticity values, the point (0.33, 0.33) represents the white color, showed below figure 1.6. Because of containing brightness data and moves the color space to a two-dimensional plane, it is easy to process and recover the data in CIE xyY color space [76].

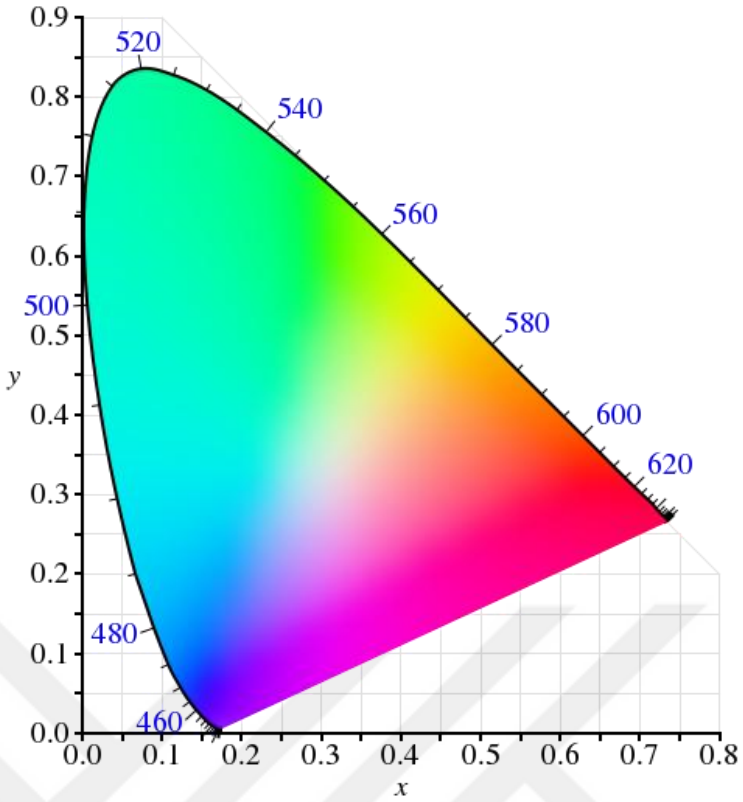

Figure 1.6 : CIE 1931 xy color space diagram.

1.4.3. CIE Lab color space

The CIE Lab color space has become the globally approved colorimetric reference system for measuring and transmitting color in 1976 and published by CIE in the same year. CIE Lab is the reference color space used by the papermaking and graphic art industries. The CIE Lab is the basis for color management and is the ICC (International Color Concercium) profile connection area, which is usually used for gamut mapping. [77]. The base of processing principle of the CIE Lab color space is to stimulate cone cells as in the same RGB and to determine the brightness of the color. One of the three different components in the CIE Lab color space gives information about lightness, one gives information about redness greenness and finally the other component gives information about blueness yellowness. CIE Lab is a coordinate system that contains all the colors in the visible spectrum and defines a color defined in this space with three components. In the three dimensional coordinate system, the chromatic a* axis lengthen from green (-a*) to red (+a*), and the chromatic b* axis lengthen from blue (-b*) to yellow (+b*). The lightness dimension, named by L*, enlarged from 0 (black) to 100 (white), as shown in figure 1.7. The point at which the a* and b* axes cross, at the L* value of 50, is neutral gray

[78]. The leveling and limits of the a* and b* axes will be bound up the specific implementation but they generally run in the range of −128 to +127. The CIE Lab color space was root from the prior "master" CIE 1931 XYZ color space, which foreseen which spectral power distributions will be comprehended as the same color but is not especially conceptually uniform [78].

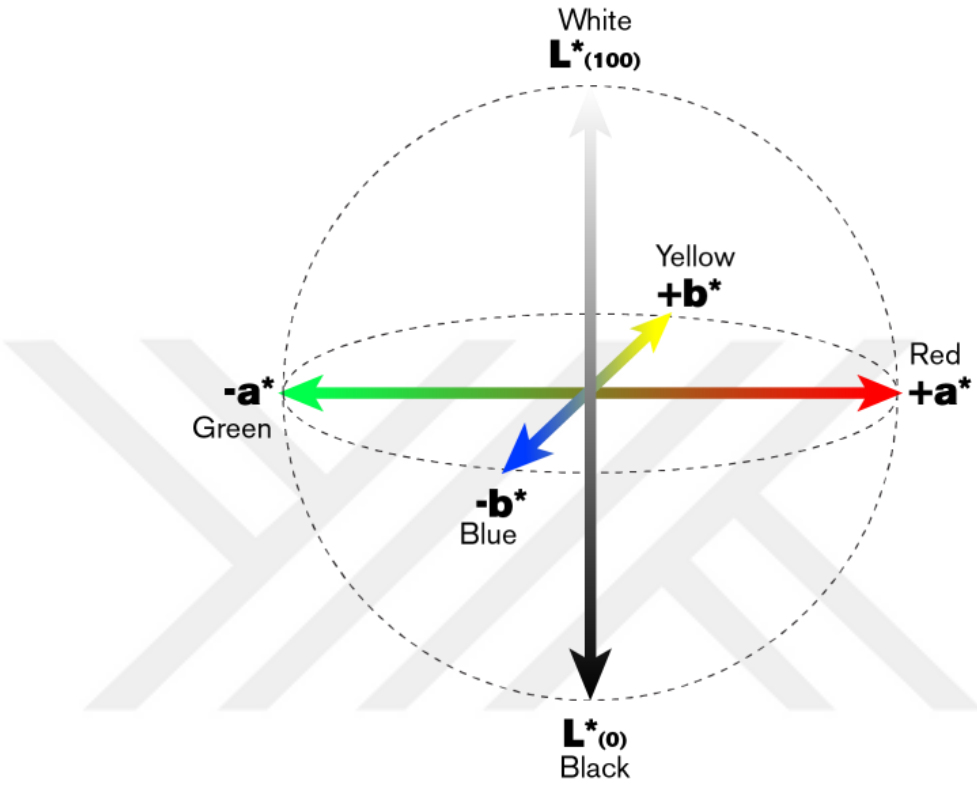

Figure 1.7 : CIE Lab color space.

Color changes can be measured as the relative distance between two reference points within a color space. This difference is typically expressed as delta E (ΔE) and is calculated by comparing reference and sample L*a*b* values how far apart two colors reside within the color space. Delta E calculations will quantify the magnitude of a color difference but do not necessarily predicate the direction of the difference [79].

$$L^* = 116\, f\left(\frac{Y}{Y_n}\right) - 16$$

$$a^* = 500\left(f\left(\frac{X}{X_n}\right) - f\left(\frac{Y}{Y_n}\right)\right)$$

$$b^* = 200\left(f\left(\frac{Y}{Y_n}\right) - f\left(\frac{Z}{Z_n}\right)\right)$$

$$\Delta L = L_{sample} - L_{standard}$$

$$\Delta a = a_{sample} - a_{standard}$$

$$\Delta b = b_{sample} - b_{standard}$$
$$\Delta E = \sqrt{(\Delta L)^2 + (\Delta a)^2 + (\Delta b)^2} \quad (1.7)$$

A positive sign for delta L* indicates that the brightness of the sample is greater than the standard, and a negative sign indicates that the sample is darker than the standard. The sign of the delta a*, positive mark denotes that the sample is more red than the standard, and a negative sign denotes that the sample is greener than the standard. When the b* value of the sample is higher than the standard, the delta b* value is positive and the yellow color is dominant. The blue color is more intense when delta b* is negative.

2. MATERIALS AND METHODS

In the present study, most commonly used colors of tattoo inks were used: blue, green, red, yellow, black, and white. In each method, tattoo dyes were treated with cold atmospheric plasma treatment in the form of liquid or agarose gel.

2.1. Cold Atmospheric Plasma (CAP) Treatment

In this study, DBD cold atmospheric plasma was obtained microseconds by using an AC pulsed power supply. Plasma treatment was performed at 2.5 kHz and 31.5 kV at 2 mm discharge range. The DBD plasma electrode's dimensions are; 6 cm and 8.5 cm. And the copper surface dimensions of DBD electrode are; 3.7 cm, 6.2 cm. Application for liquid samples was made in glass containers with 3 cm, 5.5 cm and 1 mm. And the agarose gel samples were placed on a glass slide in such a way that the samples do not exceed the dimensions of DBD electrode and plasma treatment was performed.

2.2. Cold Atmospheric Plasma (CAP) Treatment on Tattoo Dye

Cold atmospheric plasma treatment was carried out with parameters which were explained above for 3, 5, 7, 10, and 15 min; intermittently on the same sample.

2.3. Cold Atmospheric Plasma Treatment on Liquid Form Tattoo Dye

2.3.1. Absorbance measurement of tattoo dye

Absorbance measurements were made to observe whether there was a change in pigment density before and after cold atmospheric plasma treatment of tattoo dyes. Dilution of various concentrations (%1, %0.5, %0.1, %0.01, %0.0075, %0.005, %0.001, %0.0001) were made for 6 different color tattoo dyes and the absorbance values between 190 and 900 nanometers were recorded on the spectrophotometer (T70 UV-Vis Spectrophotometer, PG Instruments Limited, Leicestershire, United Kingdom). Absorbance spectrum values were determined as a result of literature

review made with tattoo dyes on laser applications. Concentration at 0.01% tattoo dyes were determined specifically because of color specific peaks on absorbance spectrum were clearly shown on this concentration. Cold atmospheric plasma treatment was carried out to tattoo dyes for 5, 7, 10, and 15 minutes duration time after the decision of tattoo dye concentration was made. For each color of tattoo dye, the absorbance values between 190 and 900 nm were compared before and after plasma treatment and then for subsequent steps duration time was determined as 15 minutes.

2.3.2. Reflectance measurement of tattoo dye

In this step, reflectance characteristics of tattoo dyes were investigated after and before cold atmospheric plasma treatment for different concentrations and time intervals. Dilution of various concentrations (%1, %0.5, %0.1, %0.01, %0.0075, %0.005, %0.001, %0.0001) were made for 6 different color tattoo dyes and the reflectance values between 400 to 900 nm wavelength were recorded on the spectrophotometer. Cold atmospheric plasma treatment was carried out to tattoo dyes for 5, 7, 10, and 15 minutes duration time after the decision of tattoo dye concentration was made.

2.4. Cold Atmospheric Plasma Treatment on Tattooed Agarose Gel

Agarose gel tests were started after the selection of tattoo dye concentration as %0.01 which showing the characteristic graphs according to the different colors on absorbance and reflectance measurements. While agarose gel is prepared, the tattoo dyes were mixed with 15 g/l hot agar (05039-500G Sigma-Aldrich®) to have %0.01 concentration of tattoo dye and poured into petri dishes with 3 mm thickness. Before the plasma was applied, tattoo dyed agarose gels were cut into squares of 1 cm to 1 cm and exposed to the plasma for 15 minutes. The other 6 color tattoo dyed agarose gel groups were exposed to plasma in two 15-minute sessions to mimic the multiple sessions of laser tattoo removal in practice.

A setup was designed to observe the color change after plasma treatment of tattoo dyed agarose gels (Figure 2.1). A black cardboard with a 2-mm thickness has been employed that does not receive any light except for the LED illumination that completely covers the lower surface. At the bottom, a surface LED (127 mm x 95 mm, Lumex Opto Components Inc., Illinois, USA) with a working voltage of 3.5 V

is placed. A drawer (9 cm x 13 cm) was designed to carry multi well plate (8.5 cm x 12.5 cm) over 1 cm of surface LED lighting. A platform was placed on the center of the camera of the phone to be used up to 9 cm from the drawer. Dimensions of weight, length, and height of the setup taken from the outside surface: 10 cm x 15 cm x 17 cm. The setup as described above has been designed to take photos of liquid or agarose gel form of tattoo dye by transferring to the multi plate, unaffected by ambient light and shadows.

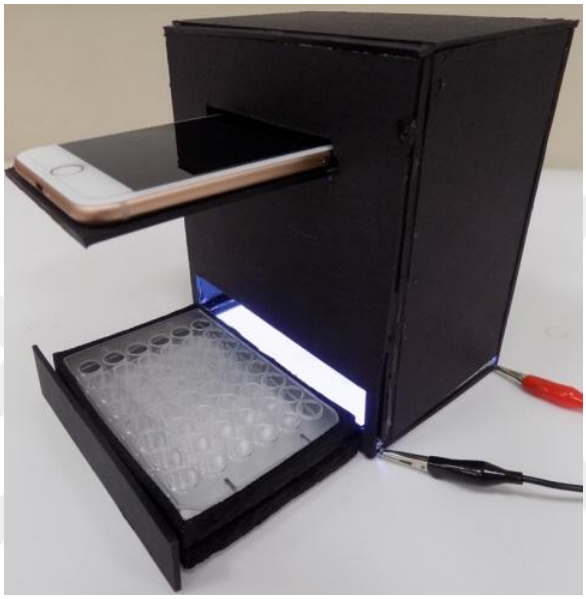

Figure 2.1 : Figure of the photographing setup.

Control group consisting of untreated tattoo dyed agarose gels and with 15 minutes and twice 15 minutes plasma treated two experimental groups were photographed by the setup. Photographed agarose gel samples were transferred to MS Paint and used the 'pick color' feature of the program and obtained the RGB value from the desired point. RGB values of photographed tattoo dyed agarose gels were converted to CIE Lab and CIE Yxy values. Conversion was provided through web sites that convert RGB values to CIE Lab and CIE Yxy values (http://colormine.org). Five RGB data from each sample were taken and necessary conversions were made. On the other hand, plasma untreated tattoo dyed agarose gels were photographed by diluting one to ten percent starting from 0.01% concentration (Figure 2.2). This process was applied separately for each color. Afterwards, the intersection points of the plasma groups were calculated by converting the RGB values of tattoo dyed agarose gels which were diluted one tenth to the CIE Yxy values. The overlapping points in the CIE Yxy color space give information about the color change of the plasma group

compared to the control group. The overlapping points in the CIE Yxy color space are also provided in RGB and CIE Lab spaces. CIE Yxy color space is interpreted over the opening of the percentage color while in CIE Lab space redness-greenness, blueness-yellowness and brightness in terms of differences between the plasma and control group has been interpreted.

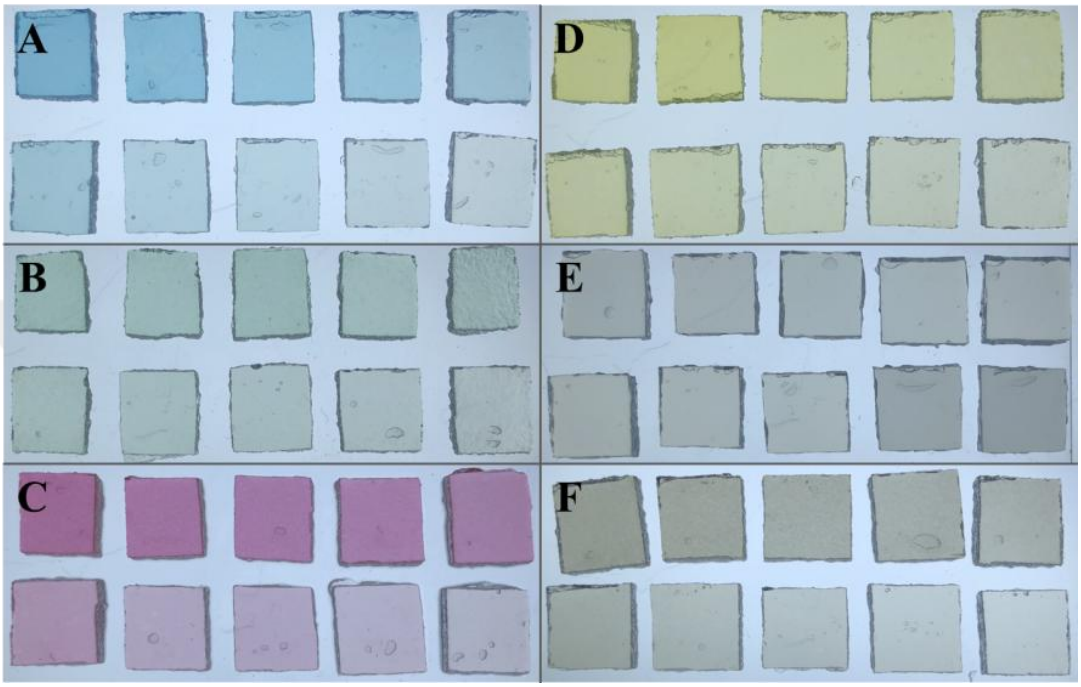

Figure 2.2 : Tattoo dyed agarose gel figures with %0,01 concentration diluted at a rate of 1/10 percent each time. The dilution sequence starting with the upper left corner and ends at the bottom right corner, for each color indicated by the letters (A:Blue, B:Green, C:Red, D:Yellow, E:White, F:Black).

2.5. Application of Cold Atmospheric Plasma Treated Distilled Water on Tattoo Dye

6 different colors of tattoo dye were prepared in 1 mL volumes at a concentration of 0.01%. Samples were transferred in 1.5 mL micro centrifuge tubes and centrifuged for 10 min at 10000 rpm (Hettich® MIKRO 120). In control groups, the supernatant is removed after centrifugation and then 1 milliliter of distilled water was added. In plasma groups, plasma treated distilled water (PT-DIW) was added instead of supernatant liquid after centrifugation. Plasma treatment was continued for 15 minutes. The difference between the control group and the plasma groups is based on the observations of the plasma treated water immediately after addition (0 hour) to the tattoo dye, 24 hours, 48 hours and 72 hours. The observations were extended by

changes in color spaces (RGB, CIE Lab, CIE Yxy) of tattoo dyes, pH measurements and absorbance change of KI solution according to the concentration of reactive oxygen species (ROS).

2.5.1. Color space changes on plasma treated distilled water applied tattoo dye

Control and plasma groups prepared as described above and they were taken to a 48 well plate and photographed by the setup used in tattoo dyed agarose gel experiments. RGB values obtained from the photos were converted to CIE Lab values and it shows the difference of color intensity of plasma group according to control group. Five RGB data from each sample were taken and CIE Lab, CIE Yxy conversions were made. It has been tried to understand how much color has been faded and the which colors are more successful than the others depending on time, on behalf of color density between plasma groups and control group by calculating delta E from CIE Lab color space.

In addition to the CIE Lab color space, tattoo dye removal was also studied in CIE Yxy space. In CIE Yxy color space comparison, control group and plasma group with the state of 72 hours after the addition of PT-DIW to the tattoo dye were placed. The largest distance from CIE Yxy color space between control and plasma group indicates which tattoo dye is faded more.

2.5.2. pH measurements of plasma treated distilled water applied tattoo dye

pH measurements of the tattoo dyes have been done after centrifuging and adding distilled water or PT-DIW to their groups. Three samples from each tattoo dye groups and subgroups were prepared and measured.

2.5.3. Absorbance change of potassium iodide (KI) solution of plasma treated distilled water applied tattoo dye

KI solution was prepared with 60 mg of potassium iodide and 30 mg of starch for 10 ml of distilled water. The control group and plasma groups (immediately after the addition of PT-DIW, after 24 hours, after 48 hours and after 72 hours) were again centrifuged at 10000 rpm for 10 minutes and then the remaining fluid was removed. After removal of the liquid on the specimens, 1 ml of KI solution was added to each sample and the solution was anticipated to change color for 30 minutes. At the end of 30 minutes, the absorbances of the specimens were measured at 680 nm. Absorbance

measurements were performed three times for each sample. The KI solution, which has a blurry white color because of containing starch, is expected to turn into a dark purple color in samples where the reactive oxygen species are intensely present.

3. RESULTS

3.1. Cold Atmospheric Application (CAP) on Liquid Form Tattoo Dye

3.1.1. Absorbance measurement of tattoo dye

The absorbance values of 6 different color tattoo dyes between 190 and 900 nm were measured at various concentrations (%1, %0.5, %0.1, %0.01, %0.0075, %0.005, %0.001, %0.0001). The concentration of %0.01 tattoo dye was chosen which gave characteristic peaks according to each color. Tattoo dyes at this concentration was exposed to plasma treatment for 5, 7, 10 and 15 minutes and again absorbance was measured between 190 and 900 nm. After measurement, it has been observed that 15 minutes plasma treatment time cause more color fading than others.

3.1.2. Reflectance measurement of tattoo dye

Reflectance measurements were performed at 400-900 nm at various concentrations (%1, %0.5, %0.1, %0.01, %0.0075, %0.005, %0.001, %0.0001) of 6 different colors of tattoo dye. Reflectance values were observed in parallel with the experiments made with tattoo dye in the literature at 0.01% concentration. At this concentration, tattoo dyes were treated plasma for 5, 10, and 15 minutes. Reflectance graphs of all tattoo dye colors after plasma treatment, it was observed that 15 minutes plasma treatment causes more color to be faded (Figure 3.1, Figure 3.2). After 15 minutes of plasma treatment reflectance of green and black colored tattoo dyes were increased compared to the control group; blue, red and white colors were reduced. There is almost no difference in reflectance between the plasma and control group of yellow color tattoo dye (Figure 3.3).

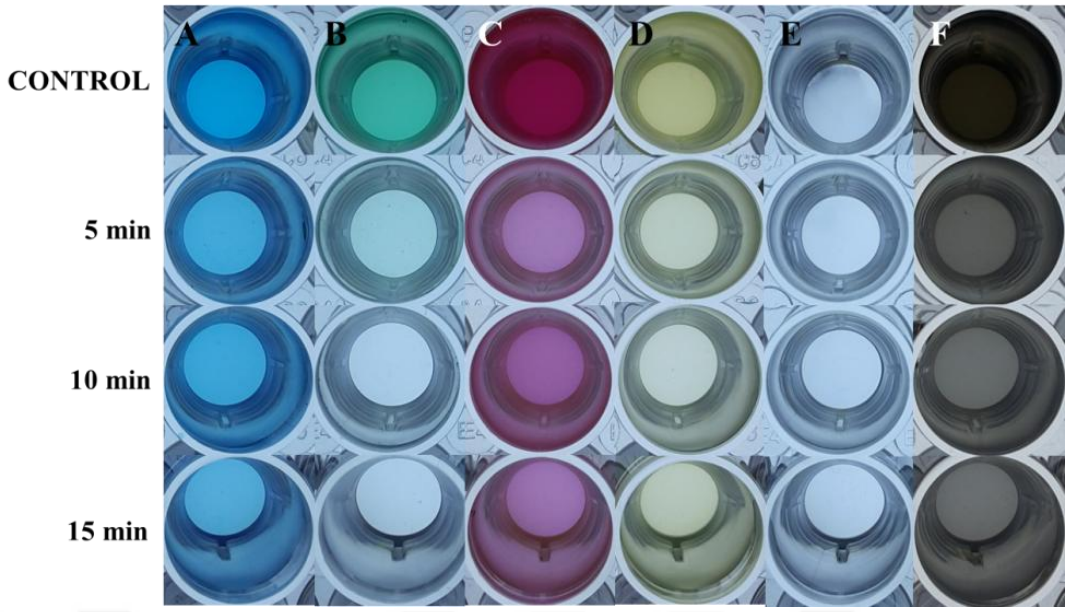

Figure 3.1 : Figure of of blue (A), green (B), red (C), yellow (D), white (E) and black (F) tattoo dyes with concentration of 0.01% in multi well plate. Each group starts from the top respectively; control group, 5 min plasma treated tattoo dye, 10 min plasma treated tattoo dye, 15 min plasma treated tattoo dye.

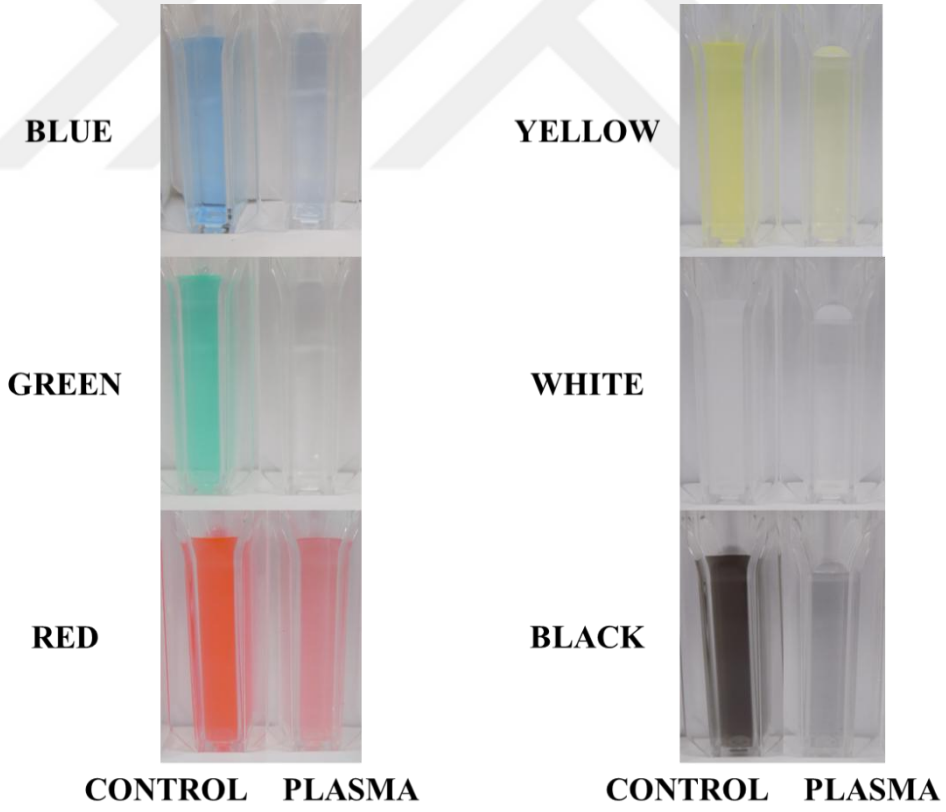

Figure 3.2 : Tattoo dyes with 0.01% concentration in 1 ml cuvettes that was not photographed in the setup, the left side of images are control groups (untreated with plasma) and the right sides are 15 min plasma treated samples.

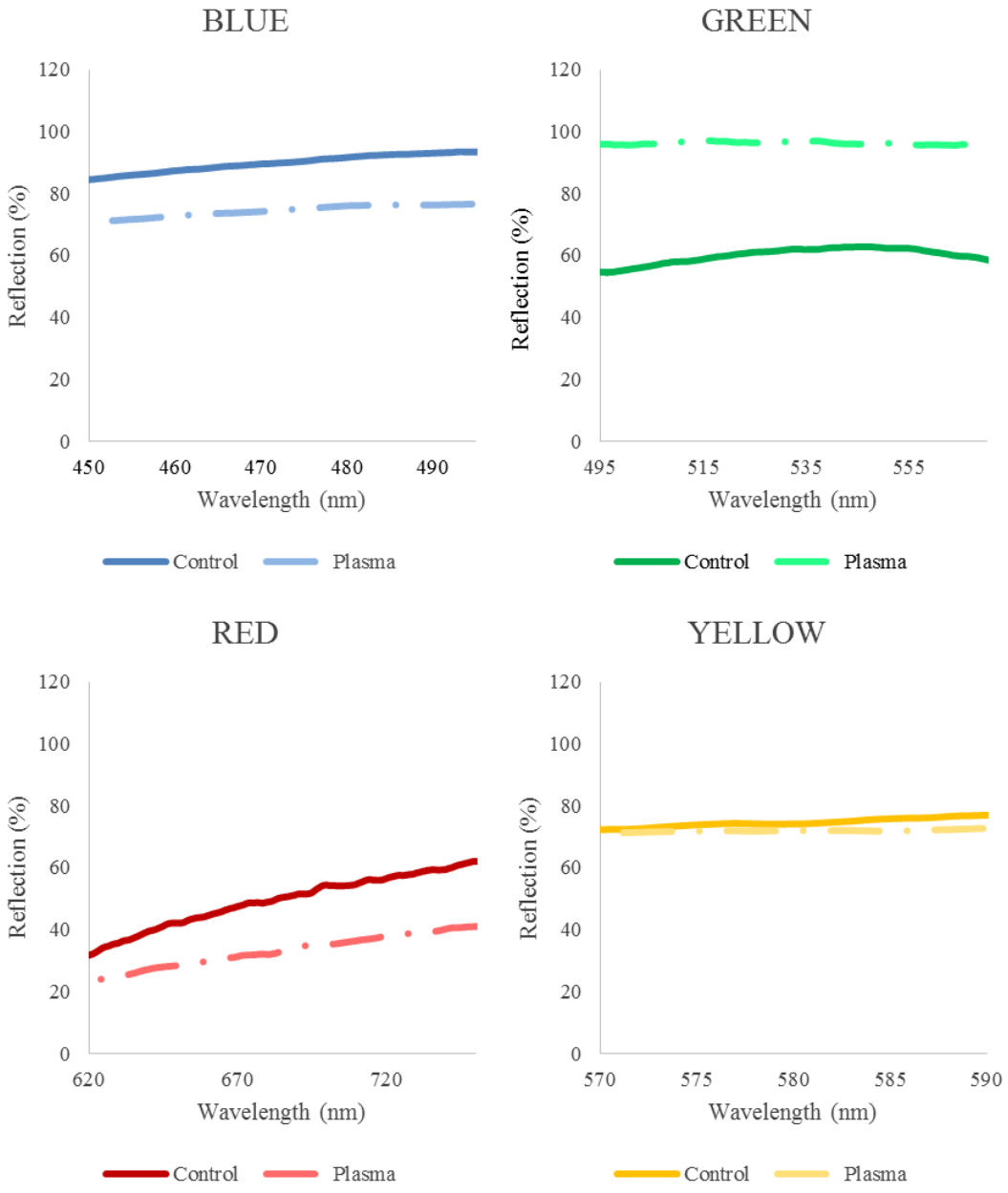

Figure 3.3 : Comparison of the reflectance values of the tattoo dyes with 0.01% concentration after 15 minutes plasma treatment (Plasma) and control group (Control). Reflectance spectrum of colors are: 450-495 nm (blue), 495-570 nm (green), 570-590 nm (yellow), 620-750 nm (red), 400-900 nm (white and black).

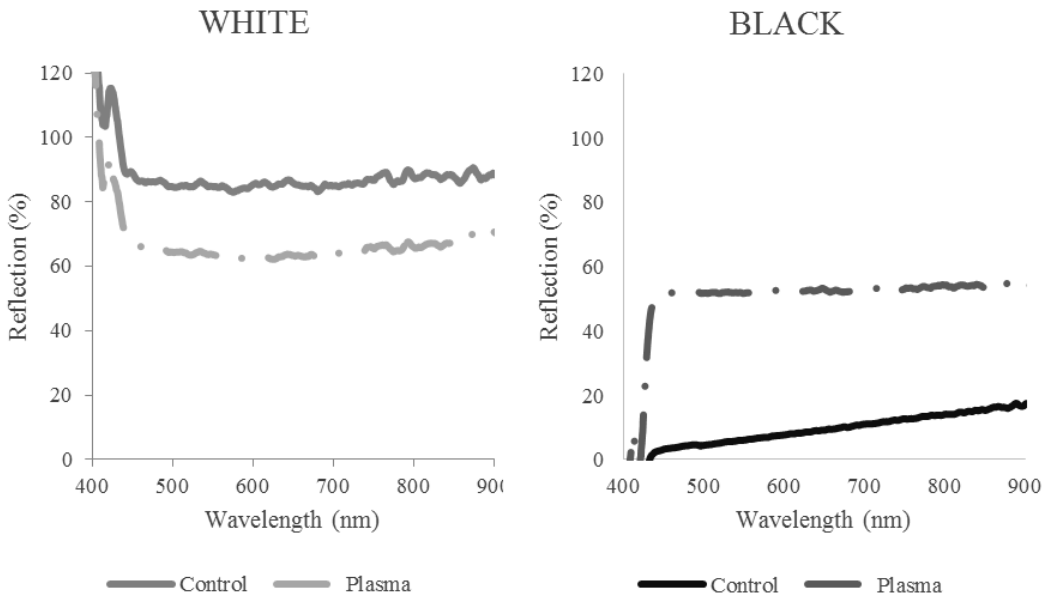

Figure 3.3 (continuation): Comparison of the reflectance values of the tattoo dyes with 0.01% concentration after 15 minutes plasma treatment (Plasma) and control group (Control). Reflectance spectrum of colors are: 450-495 nm (blue), 495-570 nm (green), 570-590 nm (yellow), 620-750 nm (red), 400-900 nm (white and black)

3.2. Cold Atmospheric Plasma Treatment on Tattoo Dyed Agarose Gel

Tattoo dyed agarose gels with a concentration of 0.01% were exposed to plasma for 15 minutes and the RGB datas were obtained by taking photographs in the setup (Figure 3.4). These values, which contain the data of the plasma group, were investigated by comparing the control group with tattoo dyed agarose gel obtained by diluting %10 ratio. The overlapping of plasma group and agarose gels prepared with 10% dilutions was examined in CIE Yxy color space (Figure 3.5). According to this experiment in CIE Yxy color space, white color tattoo dyed agarose gel was faded at 20%; blue, green, and yellow tattoo dyed agarose gels were faded at %40; black and red tattoo dyed agarose gels were faded their color at %70 according to control group. The graphs of CIE Yxy color space where the above percentage change in color is calculated are shown in Figure 3.6.

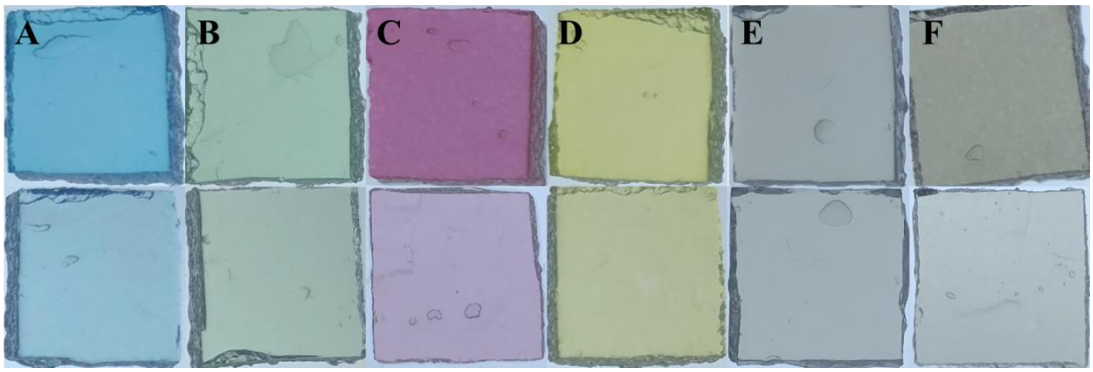

Figure 3.4 : Tattoo dyed agarose gels with concentration of 0.01%. First line of the image consists of control groups of agarose gels. The second line shows 15 minutes plasma treated samples (A:Blue, B:Green, C:Red, D:Yellow, E:White, F:Black).

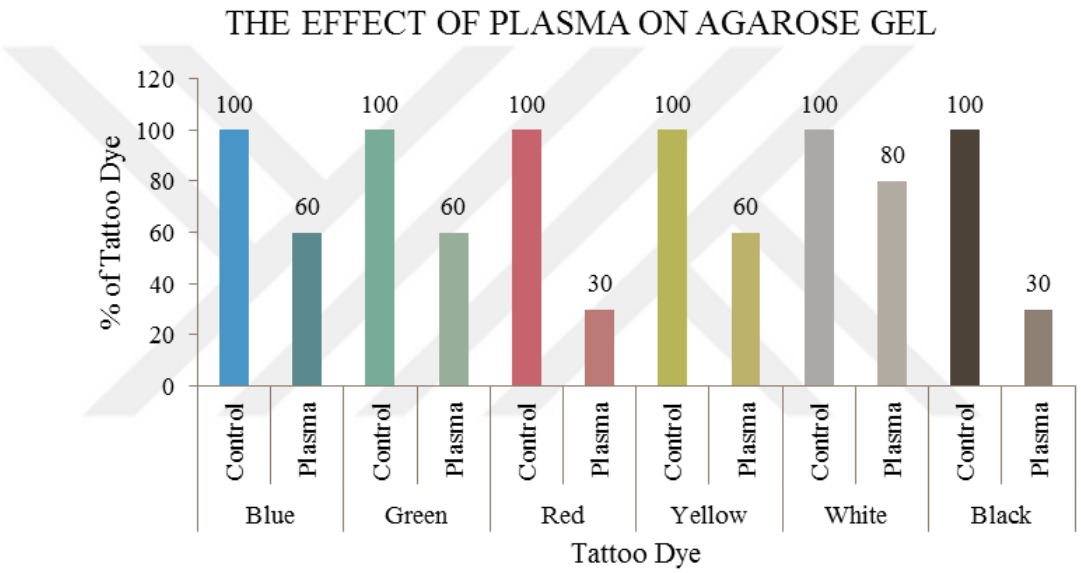

Figure 3.5 : The control groups of each tattoo dyed agarose gel were assumed to have a 100% saturation. The color intensity of agarose gels after 15 minutes of plasma treatment was calculated with the values in the CIE Yxy color space.

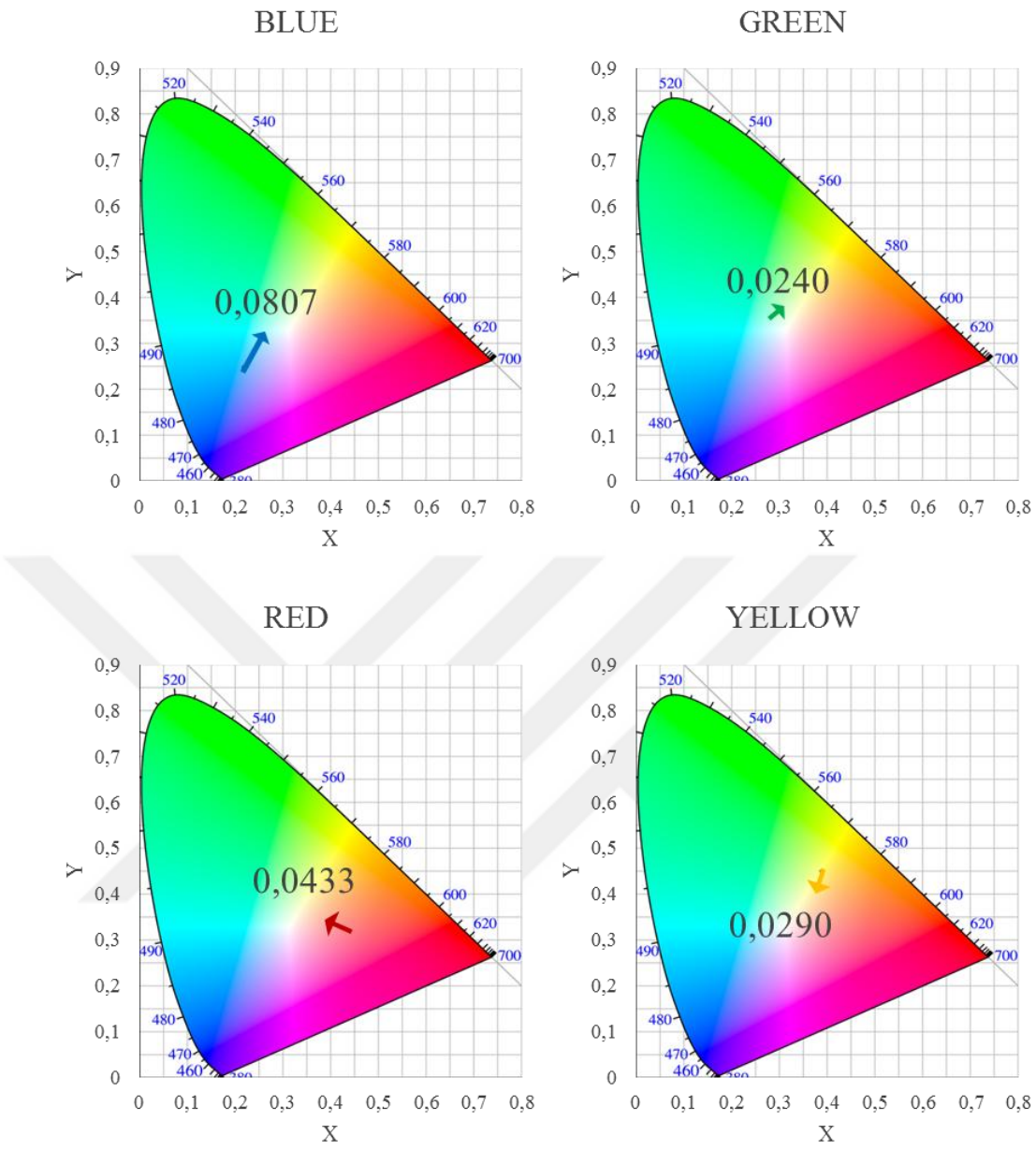

Figure 3.6 : Coordinate of tattoo dyed agarose gels with 0.01% concentration in CIE Yxy color space. The starting points of the arrows in the graphs show the coordinates of the control groups of each color. And the end points were indicated their position plasma treated samples for 15 minutes. The values next to the arrows indicate the displacement between the starting and ending points, i.e. the absolute color change between the plasma and control groups.

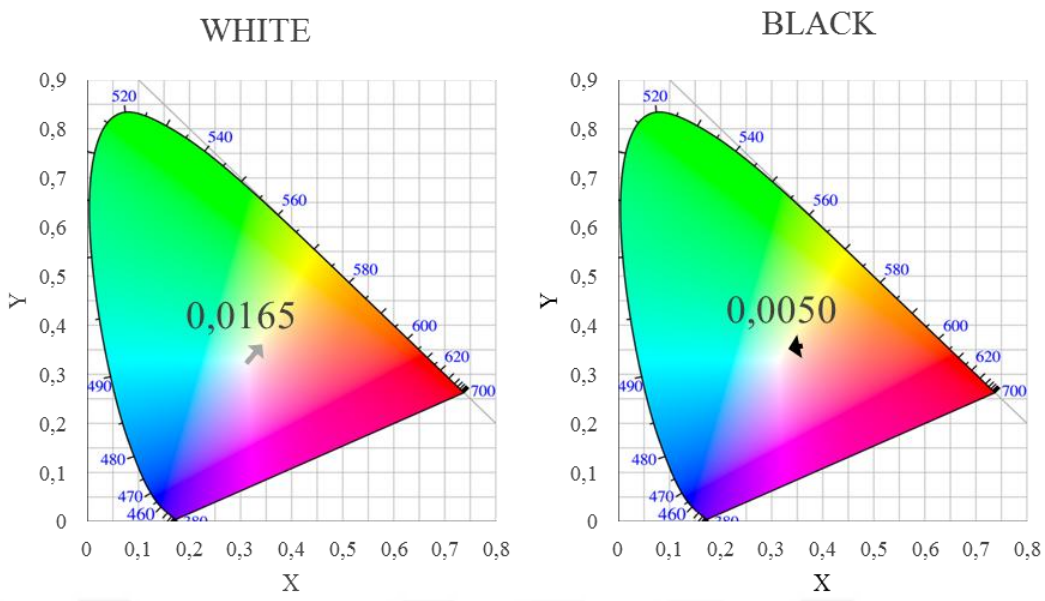

Figure 3.6 (continuation): Coordinate of tattoo dyed agarose gels with 0.01% concentration in CIE Yxy color space. The starting points of the arrows in the graphs show the coordinates of the control groups of each color. And the end points were indicated their position plasma treated samples for 15 minutes. The values next to the arrows indicate the displacement between the starting and ending points, i.e. the absolute color change between the plasma and control groups.

When looking at the values of tattoo dyed agarose gels in CIE Lab color space; blue, green, red and yellow in the a*-b* axis approximation of zero point was observed, that is the color intensities of tattoo dyed agarose gels were decreased. White tattoo dyed agarose gel after plasma treatment yellow coloration is observed, while black tattoo dyed agarose gel after plasma has increased brightness (Figure 3.7). Figure 3.8 shows delta E change of tattoo paints in CIE Lab space.

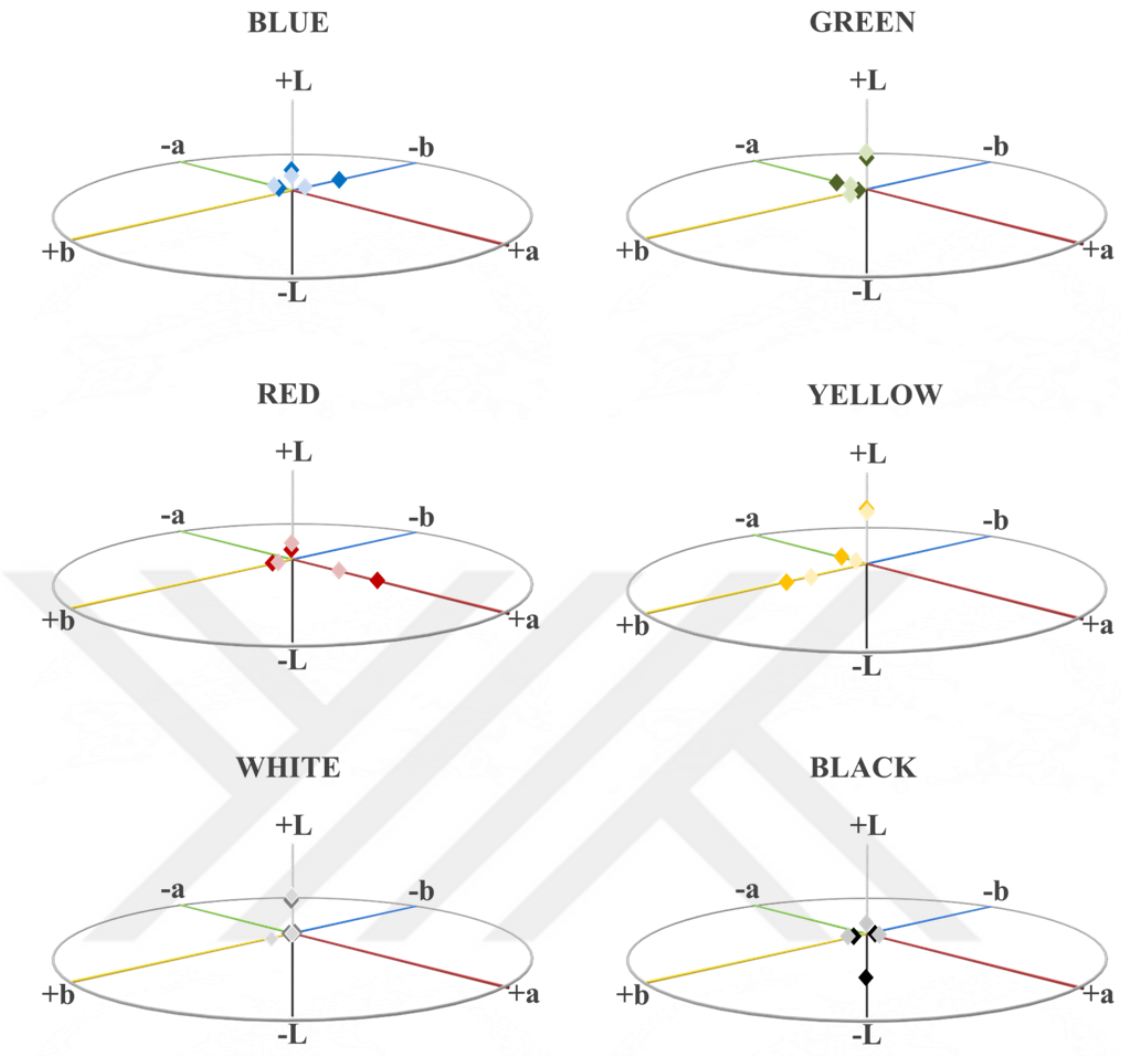

Figure 3.7 : Coordinates of tattoo dyed agarose gels with 0.01% concentration in CIE Lab color space. For L*, a*, and b* axes, there are two points on each image. The dark spots indicate the control group, while the light colored spots show 15 minutes plasma treated samples.

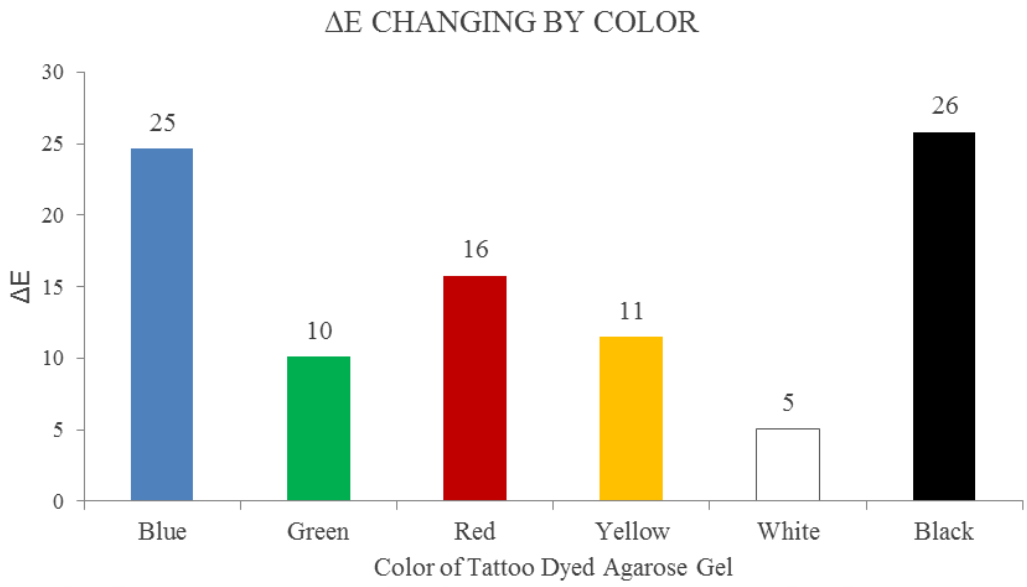

Figure 3.8 : Difference in delta e value due to color change in agarose gel after 15 minutes of plasma treatment according to control group.

3.3. Application of Cold Atmospheric Plasma Treated Distilled Water on Tattoo Dye

The indirect effects of plasma were investigated by adding plasma treated distilled water to the tattoo dye. Plasma treated distilled water (PT-DIW) caused color to be faded immediately after coming into contact with tattoo paint and increased efficiency over time. The effects of color fading as well as the effects are examined in the following titles.

3.3.1. Color space changes on plasma treated distilled water applied tattoo dye

RGB data was recorded for each sample with control group and plasma groups which they were applied with PT-DIW over time (immediately after the addition of PT-DIW, after 24 hours, after 48 hours and after 72 hours). RGB datas were converted to CIE Lab values and delta E values calculated for each color and the color intensity between control and plasma groups were investigated at which time interval (Figure 3.9). According to the data obtained; green, red, yellow and white colors were reached their maximum level of color fading after 48 hours. The maximum color fading effect of blue color was seen after 24 hours and the black color fading was seen after 72 hours. The most color fading effect was seen in red colored tattoo dye. The indirect effect of plasma in the CIE Lab color space was more common in red

and yellow, while in blue and green there was less impact. The values of L *, a *, b * which give these delta E changes are shown in figure 3.10.

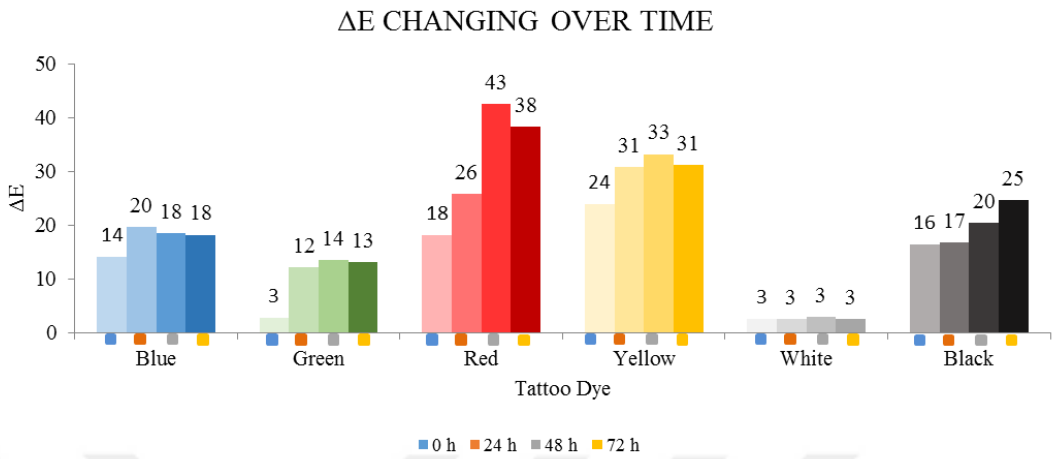

Figure 3.9 : ΔE value obtained from the CIE Lab color space of the tattoo dyes added with plasma treated water is shown in the graph above. The color codes that appear just below the bars in the graph show parallelism with the legend. In other words, it proceeds from 0 to 24 hours, 48 hours and 72 hours from left to right for each color.

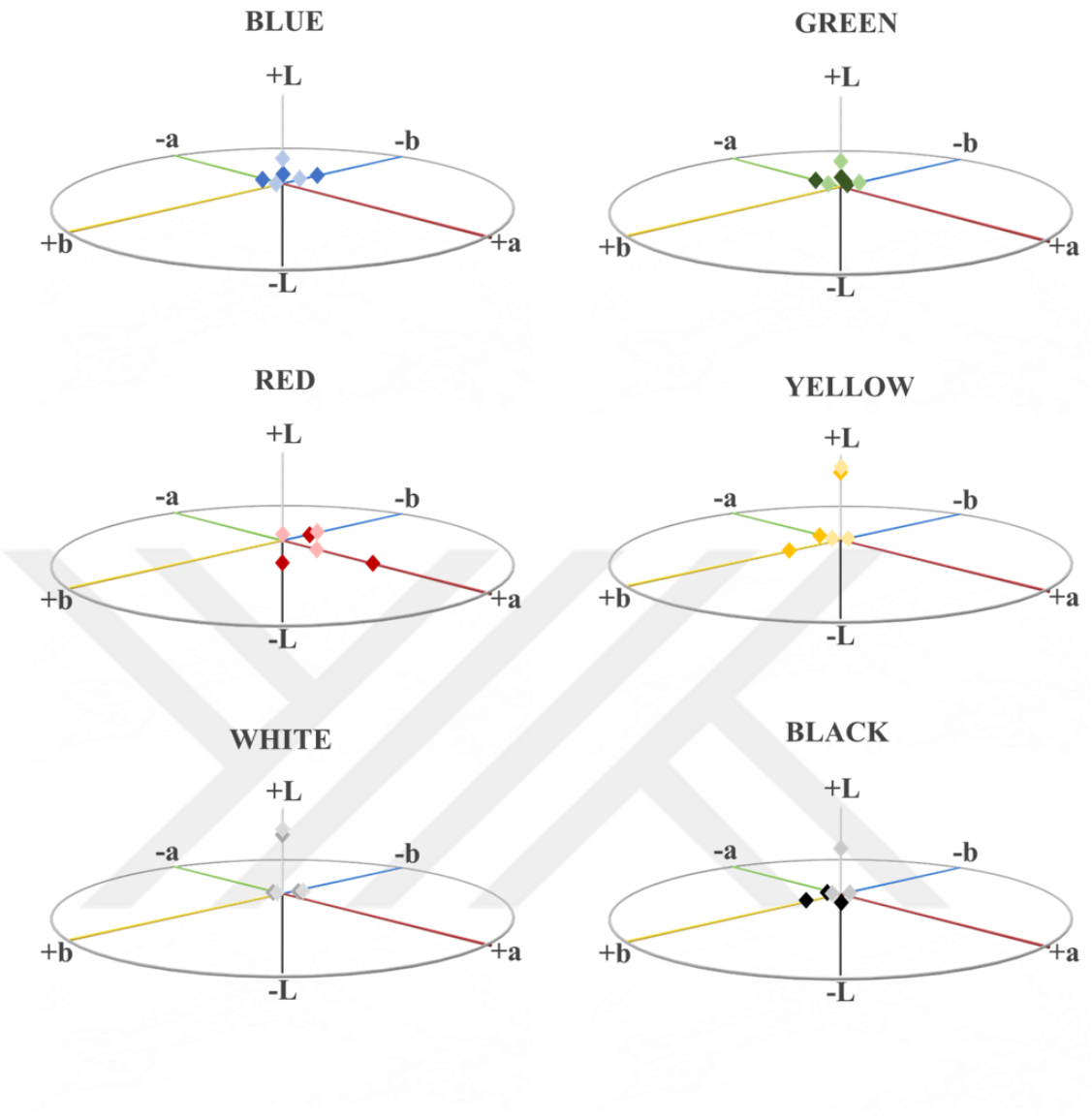

Figure 3.10 : The effect of plasma treated water on tattoo dye after 72 hours and the control group are included in CIE Lab color space for each color. For L*, a-, and b* axes, there are two points on each image. The dark spots indicate the control group, while the light colored spots show 72 hours later plasma treated water on tattoo dye.

In CIE Yxy color space, the difference between the control group and the tattoo dye that interacted with the PT-DIW for 72 hours was seen again in red color (Figure 3.11). The color fading was followed by yellow, blue, black, green and white colored tattoo dyes respectively. Figure 3.12 shows the image of the tattoo dyes that give changes in the color spaces as a result of the interaction of PT-DIW and tattoo dyes over 24-hour time intervals.

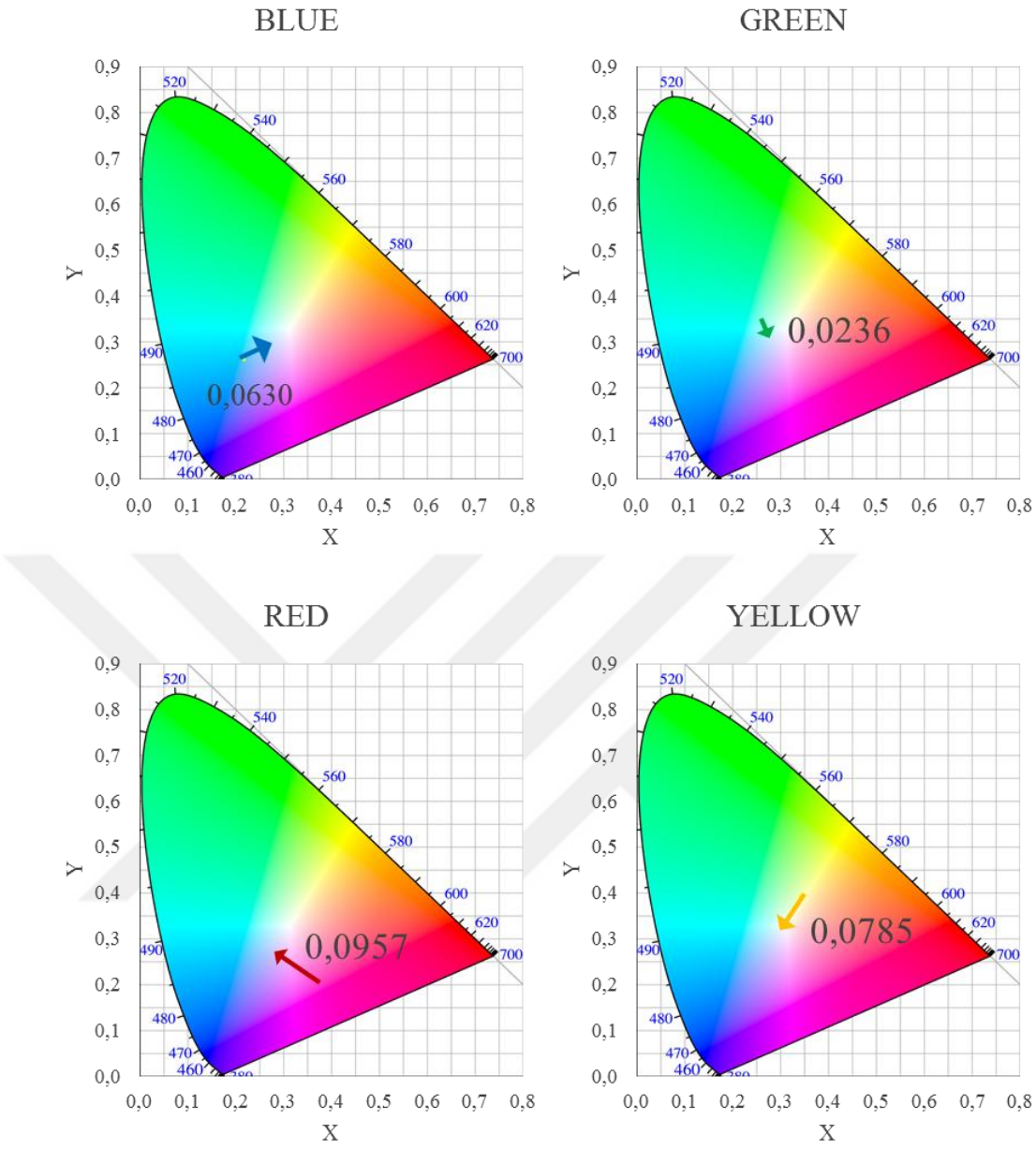

Figure 3.11 : 72 hours after the addition of PT-DIW to the tattoo dye and control group are shown above in CIE Yxy color space. The starting points of the arrows in the graphs show the coordinates of the control groups of each color. And the end points were indicated their position 72 hours after the addition of plasma treated water. The values next to the arrows indicate the displacement between the starting and ending points, i.e. the absolute color change between the plasma and control groups. All colors tend to approach white point (0.33, 0.33).

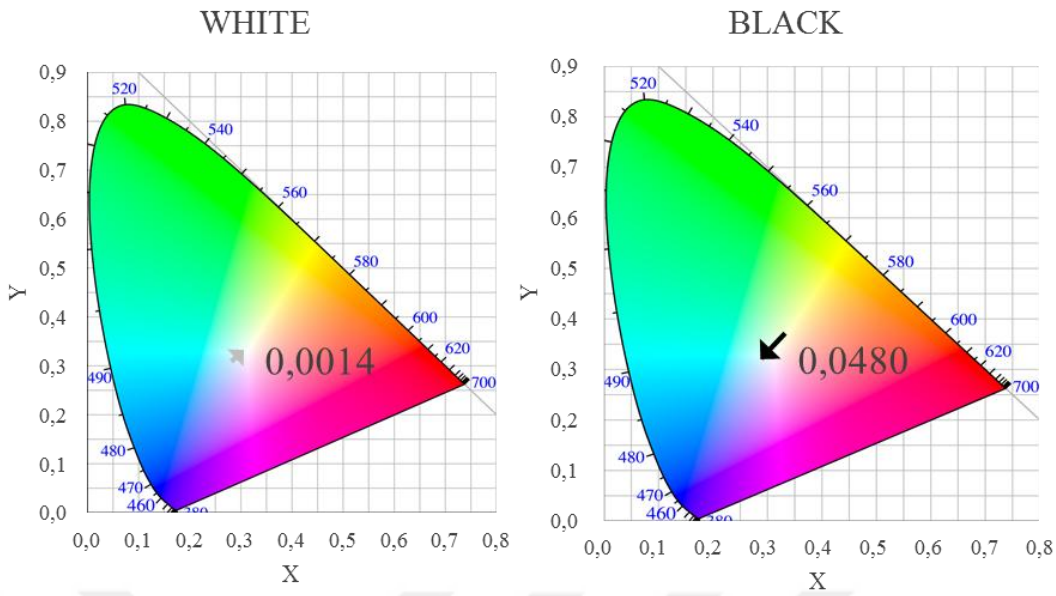

Figure 3.11 (continuation): 72 hours after the addition of PT-DIW to the tattoo dye and control group are shown above in CIE Yxy color space. The starting points of the arrows in the graphs show the coordinates of the control groups of each color. And the end points were indicated their position 72 hours after the addition of plasma treated water. The values next to the arrows indicate the displacement between the starting and ending points, i.e. the absolute color change between the plasma and control groups. All colors tend to approach white point (0.33, 0.33).

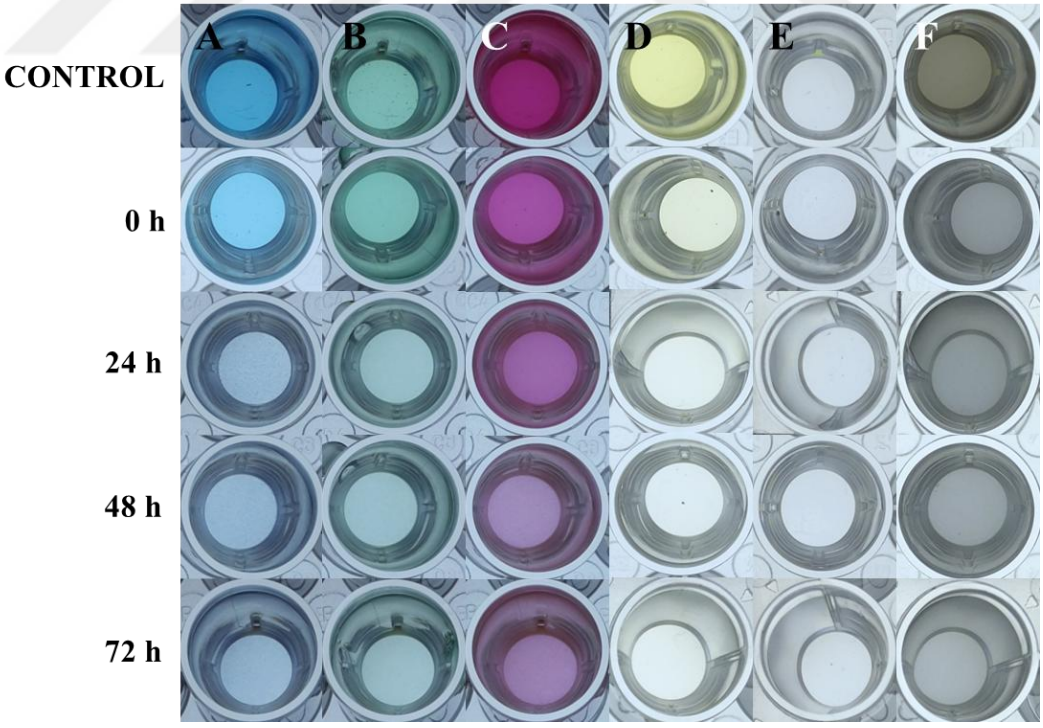

Figure 3.12 : Images of tattoo dye interacted with PT-DIW giving CIE Yxy and CIE Lab values above % in multi well plate. Each group starts from the top respectively; control group, 0 hour interaction with PT-DIW and tattoo dye, 24 hours interaction with PT-DIW and tattoo dye, 48 hours interaction with PT-DIW and tattoo dye, and

72 hours interaction with PT-DIW and tattoo dye (A:Blue, B:Green, C:Red, D:Yellow, E:White, F:Black).

3.3.2. pH measurements of plasma treated distilled water applied tattoo dye

The pH value of each tattoo dye of control group is close to neutral and ranges between 5.7 and 6.5 (Figure 3.13). The lowest pH values were measured immediately after the plasma treateds water and the tattoo paint interacted. These values range from 0.58 to 0.63. PT-DIW and the effect of tattoo dye measured pH value does not exceed 0.72 value shows tendency to unstable graph. Approximately 90% pH decrease was observed in each color according to control group and immediately after the addition of PT-DIW.

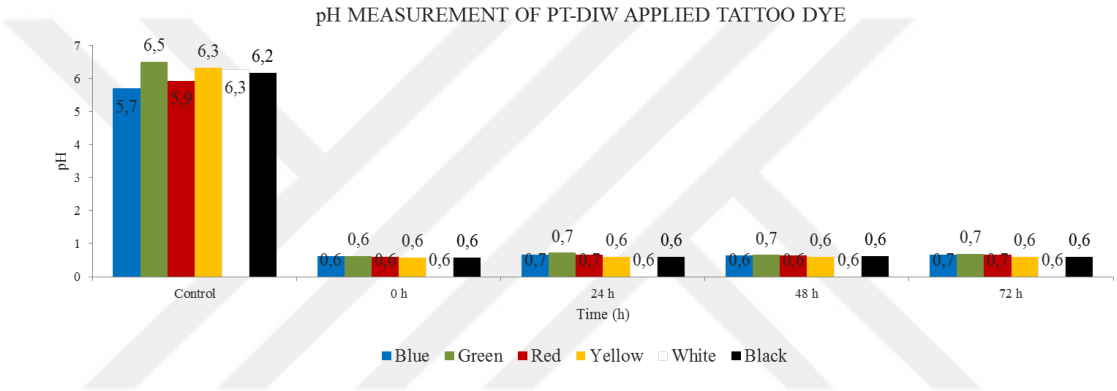

Figure 3.13 : pH graphs of control groups and 0, 24, 48, and 72 hours after the addition of PT-DIW to the tattoo dye are shown respectively.

3.3.3. Absorbance change of potassium iodide (KI) solution of plasma treated distilled water applied tattoo dye

KI solution shows dark purple coloration in the presence of reactive oxygen species. The most intense KI staining was observed immediately after the addition of PT-DIW onto the tattoo dye, and the density of reactive oxygen species and KI color density decreased over time. No purple staining was observed in any of the control groups. No correlation was observed between the color of the tattoo dyes and the color intensity of the KI solution. However, when the absorbance measurements are examined, the absorbance values decrease respectively at 680 nm; blue, green, black, yellow, red, and white colored tattoo dyes at 0. Hour (Figure 3.14). Absorbance values in all colors towards the 72th hour decreased. Reactive oxygen species were found in all colors after 72 hours. Reactive oxygen species density was observed in blue, green, yellow, black, red, and white colored tattoo dyes respectively.

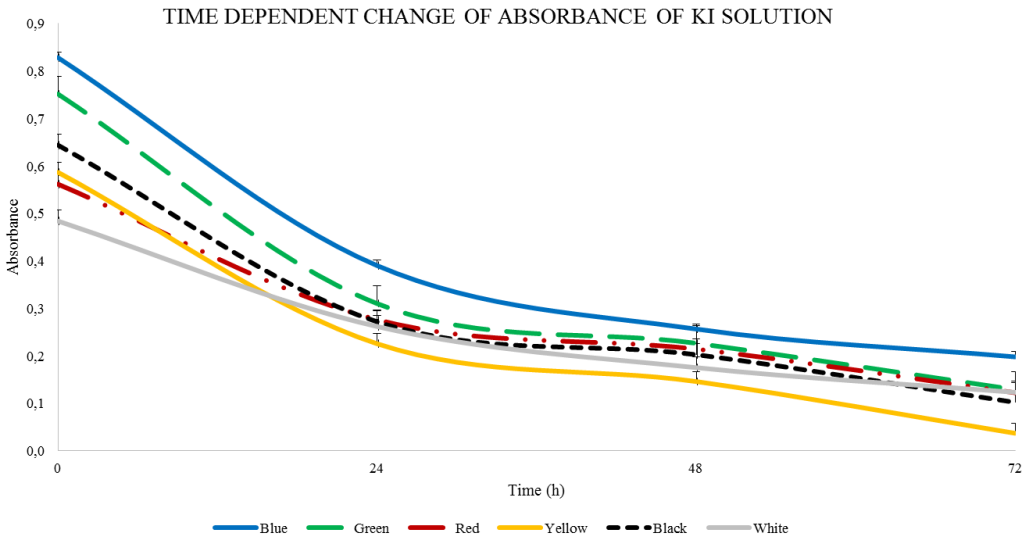

Figure 3.14 : Absorbance graph of the mixture of PT-DIW and tattoo dye with KI solution at 680 nanometers. In order to observe the difference in absorbance of the control group after the interaction with PT-DIW, the absorbance values of non-treated samples in 680 nanometers were excluded from the absorbance values after 0, 24, 48, and 72 hours.

4. DISCUSSION

Direct and/or indirect cold atmospheric plasma treatment causes discoloration or change on the material that is applied. It has been experienced in several studies that the factors causing the color fading or alteration in plasma treatment, the UV photons and the RONS components that are exposed in the plasma-generated medium, have changed the chemical composition of the tattoo pigments or have a disintegrating effect. It has been noted that the color values have changed in some studies conducted in food and agriculture to benefit from the antimicrobial activity of plasma. For example, it has been observed that reactive species released during plasma formation lead to a change in the color of meat. According to the ligands bonded by the iron atom present in myoglobin, the color of meat can be purplish, brownish or bright red. Rød *et al*. has shown that redness is reduced but there was no significant difference in b * and L * values after DBD plasma application on the ready to eat meat [80]. Kim *et al.* proved that in the presence of oxygen and when the power of cold atmospheric plasma was increased, a * and b * values increased and in dry environments a decrease in brightness was observed [81]. Yong *et al.* also perceived that myoglobin discolourization on pork, beef and chicken meat that is redness of meat has been decreased and shown to be more greenish color after cold atmospheric plasma treatments [82]. Cold atmospheric plasma is also proven to be used in dental bleaching applications in dentistry, by providing antimicrobial properties and without damaging the tooth surface [83-85]. Materials which generally produce color on the tooth surface are organic compounds which have expanded conjugated chains of alternate single or double bonds and are called chromophores containing heteroatoms, carbonyl and phenyl rings. The bleaching of the chromophore, which tends to color the teeth, can be caused by the breaking, separation or oxidation of one or more double bonds in the conjugate chain [86]. It has been observed in several studies that hydrogen peroxide, one of the reactive species formed as a result of plasma treatment, which is widely used in tooth

bleaching applications, has a whitening (increase in L* value) effect and removes yellow color (decrease in b* value) as mentioned [86-88].

In present study, various experiments have been performed on the pigment of permanent tattoo dye by benefiting from the color fading and modifying activity of cold atmospheric plasma treatment. For this purpose, tattoo dye was applied on the filter paper and cold atmospheric plasma was applied with DBD electrode for several minutes, for the first time of experimental setup. In the filter paper, water was dripped to prevent any damage during the plasma formation, and it was observed that the color of the tattoo dye was degraded in interruptedly treatment at the end of approximately 20 minutes.

The direct effects of the cold atmospheric plasma to the tattoo dye were examined in two different ways as being in liquid form and embedded in the agarose gel. In liquid state, absorbance and reflectance values of the tattoo dyes diluted in various concentrations were examined by using tattoo artist's tattoo dye diluting method. The absorbance values were measured close to 100% since the pigments were too dense which hindered most of the light falling on the particles. When measuring the absorbance, except for the intensity of the diluted tattoo dyes, another problem was the difficulty of finding the absorbance value proportional to the concentration. Due to these difficulties, the reflectance measurements of the tattoo dyes were made by detecting the reflectance value which is the wavelength of the object reflected with the reflected light. In blue, green, red and yellow tattoo dyes, it is expected that, the tattoo pigments may cause degradation of the pigment by breaking down or causing different chemical effects with the effect of plasma. In blue and green color tattoo dye, the expected effect is achieved both visually and in terms of increased reflectance. However, in yellow and red color tattoo dye, although the color opening is provided visually, there is no increase in reflectance value. Due to the characteristic of black color, when the surface absorbs the light, it looks darker [89]. Therefore, it is expected that the reflectance value of black color tattoo dye will increase. This prediction has been validated both visually and to increase of reflectance value. When it comes to white color, it is reflecting the entire spectrum in the visible region of electromagnetic spectrum [89 It is expected that there will be a decrease in reflectance after plasma treatment or fluctuations in various regions of the visible spectrum. It is expected that all colors of tattoo dye other than white will

increase compared to the reflectance control group and will draw graphs similar to water or white color. When it comes to white colored tattoo dye, it was predicted as decreasing of reflectance values which it means to increase of absorbance values and a darker color. White color tattoo dye has also shown a decrease in reflectance values as predicted, but visually, the plasma effect is not obvious.

It has been proven by various studies that the pH value has decreased and the sample surface has caused various chemical changes by the release of reactive species in the samples which interact with cold atmospheric plasma. Reddy *et al.* examined that, the oxygen-induced reactive species, especially hydrogen peroxide, hydroxyl radicals and ozone formed by DBD plasma can degrade textile dye methylene blue [90]. Tiwari *et al.* observed that as the percentage of ozone in the environment increases, a * and b * values approach to zero and the brightness increases, on carboxyl methyl cellulose, which is a high molecular weight polysaccharides [91]. At the same time, laser tattoo removal applications on darker tattoo dyes were found to be more successful results but green, yellow, white and red colors were shown to be less effective [15,92,93]. The mechanism of the laser not to fragment the melanin pigment causes dyes to be disadvantageous on yellow, yellowish green and red tattoos. In terms of reflectance spectrum, cold atmospheric plasma can be said to be more effective in degrading green color tattoo dye, compared to laser tattoo removal applications.

In tattoo removal applications, although laser is not used in UV spectrum (40-400 nm wavelength), it is seen that red and black tattoo inks cause various problems with sunlight [94]. From this point of view, the effects of sunlight and UV radiation on red tattoo dye were investigated, it was observed that the sunlight degraded the entire red color at the end of 110 days (water-like transparency) and UV radiation were removed a little of red pigments after 4 hours (yellowish color) [95]. In studies on red color tattoo dye, the components that are likely to occur after laser application are methylnitroaniline (MNA) and nitrotoluene (NT) and their cancerogenic activity has been investigated [95,96]. UV radiation-induced ROS formation is thought to cause micro and nano-sized photosensitive reactions in the skin and tattoo pigments, but best of our knowledge these studies have been performed only in red and yellow color tattoo dyes. In yellow tattoo dye, xenon arc lamp was used to mimic the sunlight and components that could cause toxic effects as a result of photochemical

lysis reactions were observed [97]. In another study with yellow tattoo dye, it was examined that the cadmium sulfide component giving pigmented color caused phototoxic effect by sunlight [98]. In the light of these studies with UV radiation, that occurs during plasma formation and do not show significant emission below 280 nm wavelength, might have thought to have a similar effect [21-23]. UV radiation generated by the plasma treatment has various effects on the surface of the skin together with the tattoo dye. The spectrum of UV radiation generated during the plasma treatment and the intensity of toxic gases (O_3, NO, and NO_2) are limited to various guidelines on dermatological applications. It does not exceed 30 J/m^2 of UV radiation in spectrum of 180-400 nm wavelengths and has a limitation for presence of toxic gases in the environment for ozone (O_3: 50 ppb), nitrogen dioxide (NO_2: 5 ppm), and nitric oxide (NO: 25 ppm) [24,25]. At the same time, studies performed with DBD plasma showed that plasma power, which may cause long-term tissue inactivation or wounds and burns, can rise above 300 J/cm^2 on human cadaver [26], and reach 120 J/cm^2 on mouse skin [27] and 540 J/cm^2 on pig skin [27] to mimic human skin.

After experiments with degradation in liquid form, agarose gel tests are the second step of direct effect of cold atmospheric plasma treatment. Tattoo dye is injected into the dermis approximately 1 mm deep from the skin surface in tattooed individuals. According to the data obtained from the literature, 1 ml tattoo dye can paint a surface of 11 cm square on the skin surface [7]. Since three of the first injected tattoo inks were placed in the dermis [7] and the tattoo artist was able to transfer only half of the dye to the skin, the concentration value of 0.01% used in our research confirms these reasons. In literature, agarose gel was chosen from gelatin and agarose gel test setups mimicking human skin by using laser on tattoo removal applications [106-108]. The penetration depth of the cold atmospheric plasma on the agarose gel embedded tattoo dye was tried to be predicted by agarose gel [109], textile dye [110] and *in vivo* experiments [109,111] in literature. Cold atmospheric plasma, which can cause up to 50 μm of apoptosis in cancer cells, has a penetration of 1.5 to 4 mm in textile products, agarose gel and animal experiments. Studies on agarose gel embedded tattoo dyes were first initiated by calculating the concentration of the plasma group by diluting the control group agarose gel. According to this step, it was observed that the tattoo dyed agarose gels which were treated for 15 minutes were mostly affected

on red and black colored tattoo dyes. A parallel activity was observed with the agarose gel embedded with black and some dark colors, which were parallel to the laser applications that showed color fading effect [15,92,93,112]. This advantage of the laser in dark colors turns into a disadvantage in iron and titanium containing compounds of pigments in colors such as white and especially skin-colored. Laser irradiation, iron-containing pigments in the presence of ferric oxide, titanium compounds in titanium dioxide compound with the interaction of the pigment will cause the pigment darkening [107,113,114]. In this study conducted with plasma, no color darkening was observed after treatment of cold atmospheric plasma in any tattoo dye.

Partial differences were observed in CIE Lab and CIE Yxy spaces when the effect of plasma on the tattoo dyed agarose gel was observed on the color spaces. In CIE Yxy color space, approaching the center to the white color, the most distant observed between plasma and control groups color was blue while the least color was black. Similar to the study with methylene blue, decrease in blue color was observed [90]. In CIE Yxy color space, since there is no data related to brightness, the comments about this data are revealed by examining CIE Lab values. The success criterions of the process in laser tattoo removal applications on color fading efficiency are usually observational [113,115-117]. In the study of cold atmospheric plasma in the field of dentistry and agriculture, the change of CIE Lab color space and delta E value has been widely used as criterion for color change [80-85]. In this study, both perspectives were used together.

Considering the criteria for fading of color in CIE Lab color space, it is anticipated that the a* and b* values will approach the center, to the zero point, and increase the brightness (L* value). The colors in which these two conditions are confirmed with green and red tattoo dyes. With these results, superiority has been established over laser applications on red and green color tattoo dye approach [15,92,93,118]. For example, in blue color tattoo dye, it was seen that the bluish effect was reduced (b* value increased) but the brightness decreased, after plasma treatment. And in yellow color dye, again the effect of yellowish decreased (b* value decreased) but the brightness decreased. In parallel with the prediction in black color tattoo dye, a very high increase in brightness was observed. In white color tattoo, a slight increase in luminosity and some yellowing effect were observed (b* value increased). When the

delta E data obtained from L*, a*, b* values are considered, the most color fading impact was seen in black and blue color tattoo dyes. In terms of results in the CIE Lab color space, plasma and laser applications have shown similarities on black and blue colored tattoo dye degredation [119,120].

The third stage of the study was to investigate the effect of plasma treated water on the degradation of tattoo dye. In CIE Yxy color space, up to 72 hours of interaction with the plasma treated water on tattoo dyes, the most degradation impact on dyes were observed on red tattoo dye while the least effect on white color. In contrast to the direct effect of plasma in CIE Lab space, in all tattoo dye colors were closed to zero-point at a*, b* values and brightness values were increased. In black color tattoo dye, the pigments of the control group showed a decrease in their b* value after the plasma treatment. In the studies on the effect of plasma treated liquids, color change was not emphasized much. These studies are using plasma for the decontamination of fruits or vegetables and declared that the color change in the products after treatment is not remarkable [121-123]. However, indirect cold atmospheric plasma treatment on meat obtained from various animals, red color increase in some applications [124,81], and decrease in some were observed [80,82]. As a result, except for color change researches of the indirect cold atmospheric plasma effect on food (in which the red color has been investigated) and the pigments used in textiles directly treated with cold atmospheric plasma, unfortunately there is not much publication.

Considering the effect of plasma treated water on pH value of tattoo dye, it was beheld that there was a decrease in pH values of tattoo dyes regardless of the color [90,125-127]. It was observed that the pH of the control group, which gave a pH value just below the neutral, decreased to level between 0.6 and 0.7 immediately after the interaction of the plasma treated water and this activity was continued for 72 hours.

In the experiment with KI solution, which change color in presence of ROS [128,129], it was realized that there was no reactive species in the control groups but they were present after the addition of plasma treated water. The existence of ROS and indirect cold atmospheric plasma treatment has been shown to be long lasting [26,44,130]. Reactive oxygen species which continued their existence by declining were the most blue in color and at least yellow at the end of 72 hours.

5. CONCLUSION

Today, the most preferred tattoo removal method with many types of applications is laser. Morover, cold atmospheric plasma has been shown to have a color fading effect in dentistry, agriculture and textiles. In present study, the efficacy of cold atmospheric plasma on the degradation of tattoo dye was investigated by combining these two fields.

When the effect of direct cold atmospheric plasma on the liquid form tattoo paint is considered, the most decisive observations were seen in green color tattoo dye and this data was confirmed with reflectance graph.

In direct plasma applied agarose gel study, the highest color degradation was observed in red and black color tattoo dyes, in CIE Yxy color space in blue and red color tattoo dyes and in CIE Lab color space in blue and black color tattoo dyes. In other words, as a result of plasma interaction with agarose gel, the colors with the most fading effect on blue, red and black colored tattoo paints, on different evaluation criteria.

When color fading feature of plasma with indirect effect is considered, the colors that are the most degraded in the CIE Yxy color space are red and yellow, and the same color is confirmed when the CIE Lab color space is examined. The various chemical reactions of the RONS components that occurred during plasma formation resulted in a decrease in pH, but no differences were observed in color-dependence. And when it was tried to be predicted by the KI solution based on the ROS concentration, the maximum absorption was observed in the blue color tattoo dye and the least in the white color.

Best of our knowledge, cold atmospheric plasma was used for the degradation of the tattoo pigments. Although visual evaluations and changes in color spaces supported each other, UV radiation and RONS components as a result of the plasma application were not fully understood. In other words, present study, which was the first trial in

this area, can be carried forward by determination of RONS components by using various analytical chemical methods and by further testing with animal experiments.

As a result, present study shows that plasma could be an alternative treatment to laser tattoo removal applications because of red, yellow and green color tattoo dyes degradation or it can be considered as an adjuvant procedure to laser tattoo removal because of its effect on the black color.

REFERENCES

[1] Velliquette, A. M., Murray, J. B., & Creyer, E. H. (1998). The Tattoo Renaissance: an Ethnographic Account of Symbolic Consumer Behavior. *NA - Advances in Consumer Research*, *25*, 461-467.

[2] Bianchi, R. S. (1988). Tattoo in Ancient Egypt. *Marks of Civilization*, Los Angeles, CA: Museum of Cultural History, 21-28.

[3] Rush, J.A. (2005). *Spiritual Tattoo: A Cultural History of Tattooing, Piercing, Scarification, Branding, and Implants.* Berkeley, California: North Atlantic Books, Chapter 1, 1-77.

[4] Ball, K. (1996). Skin and Bones: Tools of the Trade. *Tattoo, 82*, 76-79.

[5] Rubin, A. (1988). The tattoo renaissance. *Marks of Civilization*, Los Angeles, CA: Museum of Cultural History, 233-262.

[6] Winkelman, J. W., & Schmieg, M. E. (2016). U.S. Patent Application No. 15/155,750.

[7] Jacobsen, E. (Ed.). (2012). Chemical substances in tattoo ink. Miljøstyrelsen.

[8] Kaur, R. R., Kirby, W., & Maibach, H. (2009). Cutaneous allergic reactions to tattoo ink. *Journal of cosmetic dermatology*, *8*(4), 295-300.

[9] Clabaugh, W. (1968). Removal of Tattoos by Superficial Dermabrasion. *Archives of Dermatology*, *98*(5), 515.

[10] Crittenden, F. M. (1971). Salabrasion: removal of tattoos by superficial abrasion with table salt. *Cutis, 7*, 295-300.

[11] Scutt, R. W. The chemical removal of tattoos. *Br J Plast Surg. 1972, 25*(2), 189-194.

[12] Venning V. A., Colver, G. B., Millard, P. R., & Ryan, T. J., (1987). Tattoo removal using infrared coagulation: a dose comparison. *Br J Dermatol., 117*(1), 99-105.

[13] Anderson, R. R., & Parrish, J. A. (1983). Selective photothermolysis: precise microsurgery by selective absorption of pulsed radiation. *Science., 220*(4596), 524-527.

[14] Bernstein, E.F. (2006). Laser treatment of tattoo. *Clin Dermatol., 24*(1), 43-55.

[15] Bäumler, W., Eibler, E. T., Hohenleutner, U., Sens, B., Sauer, J., & Landthaler, M. (2000). Q-switch laser and tattoo pigments: first results of the chemical and photophysical analysis of 41 compounds. *Lasers Surg Med., 26*(1),13-21.

[16] Berlien, H. P., Breuer, H., Müller, G. J., Krasner, N., Okunata, T., & Sliney, D. (2012). *Applied laser medicine.* Springer Science & Business Media.

[17] Winkelman, J. W., & Schmieg, M. E. (2016). U.S. Patent Application No. 15/155,750.

[18] Grevelink, J. M., Casparian, J. M., Gonzalez, E., Momtaz, K., DeCorte, S. D., & Grassi, A. M. (1993). Undesirable side effects associated with treatment of tattoos and pigmented lesions with Q-switched lasers at 1064 nm and 694 nm: The MGH experience. *Lasers Surg Med, 131*(5), 53.

[19] Fitzpatrick, R. E., & Goldman, M. P. (1994). Tattoo removal using the alexandrite laser. *Arch Dermatol, 130*, 1508-1514.

[20] Reid, W. H., McLeod, P. J., Ritchie, A., & Ferguson-Pell, M. (1983). Q-switched ruby laser treatment of black tattoos. *British Journal of Plastic Surgery, 36*(4), 455–459.

[21] Kossida, T., Rigopoulos, D., Katsambas, A., & Anderson, R. R. (2012). Optimal tattoo removal in a single laser session based on the method of repeated exposures. *Journal of the American Academy of Dermatology, 66*(2), 271–277.

[22] Kilmer, S. L. (1993). The Q-Switched Nd:YAG Laser Effectively Treats Tattoos. *Archives of Dermatology, 129*(8), 971.

[23] Compton, K. T. (1930). KT Compton and I. Langmuir, Rev. Mod. Phys. 2, 123 (1930). *Rev. Mod. Phys., 2*, 123.

[24] Crookes W. (1983). On radiant matter spectroscopy: a new method of spectrum analysis. *Proceedings of the Royal Society, 35*, 262–267.

[25] Fridman, A. (2008). *Plasma chemistry*. Cambridge university press.

[26] Fridman, G., Friedman, G., Gutsol, A., Shekhter, A. B., Vasilets, V. N. & Fridman, A. (2008), Applied Plasma Medicine. *Plasma Processes Polym*., 5, 503-533.

[27] Fridman, G., Shereshevsky, A., Peddinghaus, M., Gutsol, A., Vasilets, V., Brooks, A., & Fridman, A. (2006, June). Bio-medical applications of non-thermal atmospheric pressure plasma. In *37th AIAA Plasmadynamics and Lasers Conference* (p. 2902).

[28] Graves, D. B. (2014). Reactive species from cold atmospheric plasma: implications for cancer therapy. *Plasma Processes and Polymers*, *11*(12), 1120-1127.

[29] MacMicking, J., Xie, QWand., & Nathan, C. (1997) Nitric oxide and macrophage function. *Annu. Rev. Immunol. 15*, 323–350.

[30] Cook, J. A., Gius, D., Wink, D. A., Krishna, M. C., Russo, A., & Mitchell, J. B. (2004). Oxidative stress, redox, and the tumor microenvironment *Semin. Radiat. Oncol., 14*, 259–66.

[31] Mander, P. K., Jekabsone, A., & Brown, G. C. (2006). Microglia proliferation is regulated by hydrogen peroxide from NADPH oxidase. *J. Immunol. 176*, 1046–1052.

[32] Polytarchou, C., Hatziapostolou, M., & Papadimitriou, E. (2005). Hydrogen peroxide stimulates proliferation and migration of human prostate cancer cells through activation of activator protein-1 and up-regulation of the heparin affin regulatory peptide gene. *Journal of Biological Chemistry*, *280*(49), 40428-40435.

[33] Sauer, H., Wartenberg, M., & Hescheler, J. (2001). Reactive oxygen species as intracellular messengers during cell growth and differentiation. *Cell. Physiol. Biochem.. 11*, 173–86.

[34] van Wetering, S., van Buul, J. D., Quik, S., Mul, F. P., Anthony, E. C., ten Klooster, J. P., Collard, J. G., & Hordijk, P. L. (2002). Reactive oxygen species mediate Rac-induced loss of cell–cell adhesion in primary human endothelial cells. *J. Cell Sci., 115*, 1837–1846.

[35] Sen, C. K., Khanna, S., Babior, B. M., Hunt, T. K., Ellison, E. C., & Roy, S. (2002). Oxidant-induced vascular endothelial growth factor expression in human keratinocytes and cutaneous wound healing. *J. Biolo. Chem., 277*, 33284–33290.

[36] Heise, M., Neff, W., Franken, O., Muranyi, P., & Wunderlich, J. (2004). Sterilization of polymer foils with dielectric barrier discharges at atmospheric pressure. *Plasmas Polymers, 9*, 23–33.

[37] Bose, B., Agarwal, S., & Chatterjee, S. N. (1990). Membrane lipid peroxidation by UV-A: mechanism and implications. *Biotechnol. Appl. Biochem., 12*, 557–561.

[38] Satoh, K., MacGregor, S. J., Anderson, J. G., Woolsey, G. A., & Fouracre, R. A. (2007). Pulsed-Plasma Disinfection of Water Containing Escherichia coli. *Japanese Journal of Applied Physics, 46*(3A), 1137–1141.

[39] Laroussi, M. (2009). Low-Temperature Plasmas for Medicine? *IEEE Transactions on Plasma Science, 37*(6), 714–725.

[40] Lukes, P., Dolezalova, E., Sisrova, I., & Clupek, M. (2014). Aqueous-phase chemistry and bactericidal effects from an air discharge plasma in contact with water: evidence for the formation of peroxynitrite through a pseudo-second-order post-discharge reaction of H_2O_2 and HNO_2. *Plasma Sources Science and Technology, 23*(1), 015019.

[41] Boudam, M. K., Moisan, M., Saoudi, B., Popovici, C., Gherardi, N., & Massines, F. (2006). Bacterial spore inactivation by atmospheric-pressure plasmas in the presence or absence of UV photons as obtained with the same gas mixture. *Journal of Physics D: Applied Physics, 39*(16), 3494–3507.

[42] Wiseman, H., & Halliwell, B. (1996). Damage to DNA by reactive oxygen and nitrogen species: role in inflammatory disease and progression to cancer. *Biochem J., 313*, 17–29.

[43] Prusiner, S. B. (1998). Prions. *Proceedings of the National Academy of Sciences*, *95*(23), 13363-13383.

[44] Kong, M. G., Kroesen, G., Morfill, G., Nosenko, T., Shimizu, T., van Dijk, J., & Zimmermann, J. L. (2009). Plasma medicine: an introductory review. *New Journal of Physics, 11*(11), 115012.

[45] Deng, X. T., Shi, J. J., & Kong, M. G. (2006). Physical mechanisms of inactivation of Bacillus subtilis spores using cold atmospheric plasmas. *IEEE Transactions on Plasma Science, 34*, 1310-1316.

[46] Klämpfl, T. G., Isbary, G., Shimizu, T., Li, Y. F., Zimmermann, J. L., Stolz, W., Schlegel, H., Morfill, G. E., & Schmidt, H. U. (2012). Cold atmospheric air plasma sterilization against spores and other microorganisms of clinical interest. *Applied and environmental microbiology*, *78*(15), 5077-5082.

[47] Fridman, G., Brooks, A. D., Balasubramanian, M., Fridman, A., Gutsol, A., Vasilets, V. N., & Friedman, G. (2007). Comparison of Direct and Indirect Effects of Non-Thermal Atmospheric-Pressure Plasma on Bacteria. *Plasma Processes and Polymers, 4*(4), 370–375.

[48] Perni, S., Shama, G., & Kong, M. G. (2008). Cold atmospheric plasma disinfection of cut fruit surfaces contaminated with migrating microorganisms. *Journal of food protection, 71*(8), 1619-1625.

[49] Fernández, A., & Thompson, A. (2012). The inactivation of Salmonella by cold atmospheric plasma treatment. *Food Research International, 45*(2), 678–684.

[50] von Woedtke, T., Metelmann, H. R., & Weltmann, K. D. (2013). Editorial–Clinical plasma medicine. *Clin Plasma Med, 1*, 1-2.

[51] Kawai, H., Shibata, Y., & Miyazaki, T. (2004). Glow discharge plasma pretreatment enhances osteoclast differentiation and survival on titanium plates. *Biomaterials*, *25*(10), 1805-1811.
[52] Shibata, Y., Hosaka, M., Kawai, H., & Miyazaki, T. (2002). Glow discharge plasma treatment of titanium plates enhances adhesion of osteoblast-like cells to the plates through the integrin-mediated mechanism. *International Journal of Oral & Maxillofacial Implants*, *17*(6), 771-777.
[53] Noro, A., Kaneko, M., Murata, I., & Yoshinari, M. (2013). Influence of surface topography and surface physicochemistry on wettability of zirconia (tetragonal zirconia polycrystal). *Journal of Biomedical Materials Research Part B: Applied Biomaterials*, *101*(2), 355-363.
[54] Shon, W. J., Chung, S.H., Kim, H.K., Han, G.J., Cho, B.H., & Park, Y.S. (2013). Peri-implant bone formation of nonthermal atmospheric pressure plasma-treated zirconia implants with different surface roughness in rabbit tibiae. *Clinical Oral Implants Research, 25*, 573-579.
[55] Simionescu, B.C., Leanca, M., Ananiescu, C., & Simionescu, C.I. (1980). Plasma-Induced Polymerization Bulk and Solution Homopolymerization of Some Vinylic Monomers. *Polymer Bulletin, 3*, 437-440.
[56] Eisner, C.B., Espey, M., Ow, H., Wang, K. W., Wiesner, U., & Schnermann, J. (2009). Measurement of Plasma Volume using Nanoparticles in Mice. *The FASEB Journal, 23*, 804-819.
[57] Southwood, L. L., & Baxter, G. M. (1996). Instrument sterilization, skin preparation, and wound management. *Veterinary Clinics of North America: Equine Practice*, *12*(2), 173-194.
[58] Ayliffe, G. (2000). Decontamination of minimally invasive surgical endoscopes and accessories. *The Journal of Hospital Infection, 45*, 263-277.
[59] Coutinho, D. S., Silveira, L., Nicolau, R. A., Zanin, F., & Brugnera, A. (2009). Comparison of temperature increase in in vitro human tooth pulp by different light sources in the dental whitening process. *Lasers in medical science*, *24*(2), 179-185.
[60] Luk, K., Tam, L., & Hubert, M. (2004). Effect of light energy on peroxide tooth bleaching. *The Journal of the American Dental Association*, *135*(2), 194-201.
[61] Yazici, A. R., Khanbodaghi, A., & Kugel, G. (2007). Effects of an In-office Bleaching System (ZOOM™) on Pulp Chamber Temperature. *J Contemp Dent Pract*, *8*, 19-26.
[62] Lee, H. W., Kim, G. J., Kim, J. M., Park, J. K., Lee, J. K., & Kim, G. C. (2009). Tooth bleaching with nonthermal atmospheric pressure plasma. *Journal of endodontics*, *35*(4), 587-591.
[63] Park, J. K., Nam, S. H., Kwon, H. C., Mohamed, A. A. H., Lee, J. K., & Kim, G. C. (2011). Feasibility of nonthermal atmospheric pressure plasma for intracoronal bleaching. *International endodontic journal*, *44*(2), 170-175.
[64] Stoffels, E., Gonzalvo, Y. A., Whitmore, T. D., Seymour, D. L., & Rees, J. A. (2006). A plasma needle generates nitric oxide. *Plasma Sources Science and Technology*, *15*(3), 501.
[65] Lademann, J., Ulrich, C., Patzelt, A., Richter, H., Kluschke, F., Klebes, M., Lademann, O., Kramer, A., Weltmann, K. D., & Lange-Asschenfeldt, B. (2013). Risk assessment of the application of tissue-tolerable plasma on human skin. *Clinical Plasma Medicine*, *1*(1), 5-10.
[66] Zaitsev, V. M. (2003). Comparative analysis of effectiveness of treatment of chronic supporated ulcers by NO-therapy with addition of ultrasound

implantation of miramistine with treatment by ultrasound implantation alone. *Russian Journal of Otorinolaringology*, *1*, 58-59.

[67] Emmert, S., Brehmer, F., Hänßle, H., Helmke, A., Mertens, N., Ahmed, R., & Schön, M. P. (2013). Atmospheric pressure plasma in dermatology: Ulcus treatment and much more. *Clinical Plasma Medicine*, *1*(1), 24-29.

[68] Fetykov, A. I., Avdeeva, E. A., Fulton, J., Ferrel, J., Gotsev, V. A., & Galov, A. A. (2009). The effectiveness of cold plasma treatment of diabetic feet syndrome, complicated by purulonecrotic process. In *Second International Conference on Plasma. San Antonio, Texas, USA*.

[69] Isbary, G., Morfill, G., Schmidt, H. U., Georgi, M., Ramrath, K., Heinlin, J., Stolz, W., & Bunk, W. (2010). A first prospective randomized controlled trial to decrease bacterial load using cold atmospheric argon plasma on chronic wounds in patients. *British Journal of Dermatology*, *163*(1), 78-82.

[70] Isbary, G., Morfill, G., Zimmermann, J., Shimizu, T., & Stolz, W. (2011). Cold atmospheric plasma: a successful treatment of lesions in Hailey-Hailey disease. *Archives of dermatology*, *147*(4), 388-390.

[71] Arndt, S., Wacker, E., Li, Y. F., Shimizu, T., Thomas, H. M., Morfill, G. E., Karrer, S., Zimmermann, J.L., & Bosserhoff, A. K. (2013). Cold atmospheric plasma, a new strategy to induce senescence in melanoma cells. *Experimental dermatology*, *22*(4), 284-289.

[72] Hunt, R. W. G. (2004). The Reproduction of Colour: Wiley-IS&T Series in Imaging Science and Technology.

[73] Wyszecki, G., & Stiles, W. S. (1982). Color science: concepts and methods, quantitative data and formulas.

[74] Smith, T., & Guild, J. (1931). The C.I.E. colorimetric standards and their use. *Transactions of the Optical Society, 33*(3), 73–134.

[75] Connolly, C., & Fleiss, T. (1997). A study of efficiency and accuracy in the transformation from RGB to CIELAB color space. *IEEE Transactions on Image Processing, 6*(7), 1046–1048.

[76] Hunt, R. W. G. (1987). *Measuring Colour*. Chichester, England: Ellis Horwood Limited.

[77] Hill, B., Roger, T., & Vorhagen, F. W. (1997). Comparative analysis of the quantization of color spaces on the basis of the CIELAB color-difference formula. *ACM Transactions on Graphics, 16*(2), 109–154.

[78] Schwarz, M. W., Cowan, W. B., & Beatty, J. C. (1987). An experimental comparison of RGB, YIQ, LAB, HSV, and opponent color models. *ACM Transactions on Graphics*, 6(2), 123–158.

[79] Connolly, C., & Fleiss, T. (1997). A study of efficiency and accuracy in the transformation from RGB to CIELAB color space. *IEEE Transactions on Image Processing, 6*(7), 1046–1048.

[80] Rød, S. K., Hansen, F., Leipold, F., & Knøchel, S. (2012). Cold atmospheric pressure plasma treatment of ready-to-eat meat: Inactivation of Listeria innocua and changes in product quality. *Food Microbiology, 30*(1), 233–238.

[81] Kim, B., Yun, H., Jung, S., Jung, Y., Jung, H., Choe, W., & Jo, C. (2011). Effect of atmospheric pressure plasma on inactivation of pathogens inoculated onto bacon using two different gas compositions. *Food Microbiology, 28*(1), 9–13.

[82] Yong, H. I., Han, M., Kim, H. J., Suh, J.-Y., & Jo, C. (2018). Mechanism Underlying Green Discolouration of Myoglobin Induced by Atmospheric Pressure Plasma. *Scientific Reports, 8*(1), 9790.

[83] Cha, S., & Park, Y. S. (2014). Plasma in dentistry. *Clinical Plasma Medicine*, *2*(1), 4–10.
[84] Pan, J., Sun, P., Tian, Y., Zhou, H., Wu, H., Bai, N., Fang, J. (2010). A Novel Method of Tooth Whitening Using Cold Plasma Microjet Driven by Direct Current in Atmospheric-Pressure Air. *IEEE Transactions on Plasma Science*, *38*(11), 3143–3151.
[85] Lee, H. W., Kim, G. J., Kim, J. M., Park, J. K., Lee, J. K., & Kim, G. C. (2009). Tooth Bleaching with Nonthermal Atmospheric Pressure Plasma. *Journal of Endodontics*, *35*(4), 587–591.
[86] Joiner, A. (2006). The bleaching of teeth: A review of the literature. *Journal of Dentistry*, *34*(7), 412–419.
[87] Joiner, A., Thakker, G., & Cooper, Y. (2004). Evaluation of a 6% hydrogen peroxide tooth whitening gel on enamel and dentine microhardness in vitro. *Journal of Dentistry*, *32*(1), 27–34.
[88] White, D. J., Kozak, K. M., Zoladz, J. R., Duschner, H. J., & Götz, H. (2000). Effects of tooth-whitening gels on enamel and dentin ultrastructure--a confocal laser scanning microscopy pilot study. *Compendium of continuing education in dentistry.(Jamesburg, NJ: 1995). Supplement*, (29), 29-34.
[89] Gouras, P., & Zrenner, E. (1981). Color vision: a review from a neurophysiological perspective. In *Progress in sensory physiology* (pp. 139-179). Springer, Berlin, Heidelberg.
[90] Manoj Kumar Reddy, P., Rama Raju, B., Karuppiah, J., Linga Reddy, E., & Subrahmanyam, C. (2013). Degradation and mineralization of methylene blue by dielectric barrier discharge non-thermal plasma reactor. *Chemical Engineering Journal*, *217*, 41–47.
[91] Tiwari, B. K., Muthukumarappan, K., O'Donnell, C. P., Chenchaiah, M., & Cullen, P. J. (2008). Effect of ozonation on the rheological and colour characteristics of hydrocolloid dispersions. *Food Research International*, *41*(10), 1035–1043.
[92] Kupermanbeade, M., Levine, V. J., & Ashinoff, R. (2001). Laser Removal of Tattoos. *American Journal of Clinical Dermatology*, *2*(1), 21–25.
[93] Levine, V. J., & Geronemus, R. G. (1995). Tattoo removal with the Q-switched ruby laser and the Q-switched Nd: YAGlaser: a comparative study. *Cutis*, *55*(5), 291-296.
[94] Hutton Carlsen, K., & Serup, J. (2013). Photosensitivity and photodynamic events in black, red and blue tattoos are common: A "Beach Study." *Journal of the European Academy of Dermatology and Venereology*, *28*(2), 231–237.
[95] Engel, E., Spannberger, A., Vasold, R., König, B., Landthaler, M., & Bäumler, W. (2007). Photochemical cleavage of a tattoo pigment by UVB radiation or natural sunlight. *JDDG: Journal der Deutschen Dermatologischen Gesellschaft*, *5*(7), 583-589.
[96] Engel, E., Vasold, R., Santarelli, F., Maisch, T., Gopee, N. V., Howard, P. C., Bäumler, W. (2010). Tattooing of skin results in transportation and light-induced decomposition of tattoo pigments - a first quantification in vivo using a mouse model. *Experimental Dermatology*, *19*(1), 54–60.
[97] Cul, Y., Spann, A. P., Couch, L. H., Gopee, N. V., Evans, F. E., Churchwell, M. I., Williams, L.D., Doerge, D.R., & Howard, P. C. (2004). Phtodeceomposition of Pigment Yellow 74, a Pigment Used in Tattoo Inks¶. *Photochemistry and Photobiology*, *80*(2), 175–184.

[98] Bjornberg, A. (1963). Reactions to Light in Yellow Tattoos From Cadmium Sulfide. *Archives of Dermatology, 88*(3), 267-271.
[99] Laroussi, M., & Leipold, F. (2004). Evaluation of the roles of reactive species, heat, and UV radiation in the inactivation of bacterial cells by air plasmas at atmospheric pressure. *International Journal of Mass Spectrometry, 233*(1-3), 81–86.
[100] Laroussi, M. (2005). Low Temperature Plasma-Based Sterilization: Overview and State-of-the-Art. *Plasma Processes and Polymers, 2*(5), 391–400.
[101] Maisch, T., Shimizu, T., Isbary, G., Heinlin, J., Karrer, S., Klämpfl, T. G., & Zimmermann, J. L. (2012). Contact-Free Inactivation of Candida albicans Biofilms by Cold Atmospheric Air Plasma. *Applied and Environmental Microbiology, 78*(12), 4242–4247.
[102] International Commission on Non-Ionizing Radiation Protection. (2004). Guidelines on limits of exposure to ultraviolet radiation of wavelengths between 180 nm and 400 nm (incoherent optical radiation). *Health Physics, 87*(2), 171-186.
[103] Center for Disease Control and Prevention (CDC) Ozone: NIOSH (National Institute for Occupational Safety and Health).
[104] Fridman, G., Peddinghaus, M., Balasubramanian, M., Ayan, H., Fridman, A., Gutsol, A., & Brooks, A. (2006). Blood coagulation and living tissue sterilization by floating-electrode dielectric barrier discharge in air. *Plasma Chemistry and Plasma Processing, 26*(4), 425-442.
[105] Dobrynin, D., Fridman, G., Friedman, G., & Fridman, A. (2009). Physical and biological mechanisms of direct plasma interaction with living tissue. *New Journal of Physics, 11*(11), 115020.
[106] Beute, T. C., Miller, C. H., Timko, A. L., & Ross, E. V. (2008). In Vitro Spectral Analysis of Tattoo Pigments. *Dermatologic Surgery, 34*(4), 508–516.
[107] Anderson, R. R., Geronemus, R., Kilmer, S. L., Farinelli, W., & Fitzpatrick, R. E. (1993). Cosmetic tattoo ink darkening: a complication of Q-switched and pulsed-laser treatment. *Archives of dermatology, 129*(8), 1010-1014.
[108] Kim, H., Hau, N. T., Chae, Y.-G., Lee, B., & Kang, H. W. (2016). 3D printing-assisted fabrication of double-layered optical tissue phantoms for laser tattoo treatments. *Lasers in Surgery and Medicine, 48*(4), 392–399.
[109] Dobrynin, D., Fridman, G., Friedman, G., & Fridman, A. (2012). Deep Penetration into Tissues of Reactive Oxygen Species Generated in Floating-Electrode Dielectric Barrier Discharge (FE-DBD): An In Vitro Agarose Gel Model Mimicking an Open Wound. *Plasma Medicine, 2*(1-3): 71–83.
[110] Wang, C. X., Ren, Y., & Qiu, Y. P. (2007). Penetration depth of atmospheric pressure plasma surface modification into multiple layers of polyester fabrics. *Surface and Coatings Technology, 202*(1), 77–83.
[111] Partecke, L. I., Evert, K., Haugk, J., Doering, F., Normann, L., Diedrich, S., Weiss, F.U., Evert, M., Huebner, N.O., Guenther, C., & Heidecke, C. D. (2012). Tissue tolerable plasma (TTP) induces apoptosis in pancreatic cancer cells in vitro and in vivo. *BMC cancer, 12*(1), 473.
[112] Leu, F. J., Huang, C. L., Sue, Y. M., Lee, S. C., & Wang, C. C. (2015). Effects of tattoo ink's absorption spectra and particle size on cosmetic tattoo treatment efficacy using Q-switched Nd: YAG laser. *Lasers in medical science, 30*(1), 303-309.

[113] Adatto, M. A., Halachmi, S., & Lapidoth, M. (2011). Tattoo Removal. *Basics in Dermatological Laser Applications, 42*, 97–110.
[114] Timko, A. L., Miller, C. H., Johnson, F. B., & Ross, E. V. (2001). In Vitro Quantitative Chemical Analysis of Tattoo Pigments. *Arch Dermatol., 137*(2):143–147.
[115] Leu, F. J., Huang, C. L., Sue, Y. M., Lee, S. C., & Wang, C. C. (2014). Effects of tattoo ink's absorption spectra and particle size on cosmetic tattoo treatment efficacy using Q-switched Nd:YAG laser. Lasers in Medical Science, 30(1), 303–309.
[116] Gómez, C., Martin, V., Sastre, R., Costela, Á., & García-Moreno, I. (2010). In vitro and in vivo laser treatments of tattoos: high efficiency and low fluences. *Archives of dermatology*, *146*(1), 39-45.
[117] Sardana, K., Ranjan, R., & Ghunawat, S. (2015). Optimising laser tattoo removal. *Journal of cutaneous and aesthetic surgery*, *8*(1), 16.
[118] Alster, T. S. (1995). Q-switched alexandrite laser treatment (755 nm) of professional and amateur tattoos. *Journal of the American Academy of Dermatology, 33*(1), 69–73.
[119] Leuenberger, M. L., Mulas, M. W., Hata, T. R., Goldman, M. P., Fitzpatrick, R. E., & Grevelink, J. M. (1999). Comparison of the Q-Switched Alexandrite, ND:YAG, and Ruby Lasers in Treating Blue-Black Tattoos. *Dermatologic Surgery, 25*(1), 10–14.
[120] Brauer, J. A., Reddy, K. K., Anolik, R., Weiss, E. T., Karen, J. K., Hale, E. K., Brightman, L.A., Bernstein, L., & Geronemus, R. G. (2012). Successful and rapid treatment of blue and green tattoo pigment with a novel picosecond laser. *Archives of dermatology*, *148*(7), 820-823.
[121] Misra, N. N., Keener, K. M., Bourke, P., Mosnier, J.-P., & Cullen, P. J. (2014). In-package atmospheric pressure cold plasma treatment of cherry tomatoes. *Journal of Bioscience and Bioengineering*, *118*(2), 177–182.
[122] Vleugels, M., Shama, G., Deng, X. T., Greenacre, E., Brocklehurst, T., & Kong, M. G. (2005). Atmospheric plasma inactivation of biofilm-forming bacteria for food safety control. *IEEE Transactions on Plasma Science*, *33*(2), 824-828.
[123] Klockow, P. A., & Keener, K. M. (2008). Quality and safety assessment of packaged spinach treated with a novel atmospheric, non-equilibrium plasma system. In *2008 Providence, Rhode Island, June 29–July 2, 2008* (p. 1). American Society of Agricultural and Biological Engineers.
[124] Fröhling, A., Durek, J., Schnabel, U., Ehlbeck, J., Bolling, J., & Schlüter, O. (2012). Indirect plasma treatment of fresh pork: Decontamination efficiency and effects on quality attributes. *Innovative Food Science & Emerging Technologies, 16*, 381–390.
[125] Xu, Y., Tian, Y., Ma, R., Liu, Q., & Zhang, J. (2016). Effect of plasma activated water on the postharvest quality of button mushrooms, Agaricus bisporus. *Food chemistry*, *197*, 436-444.
[126] Traylor, M. J., Pavlovich, M. J., Karim, S., Hait, P., Sakiyama, Y., Clark, D. S., & Graves, D. B. (2011). Long-term antibacterial efficacy of air plasma-activated water. *Journal of Physics D: Applied Physics*, *44*(47), 472001.
[127] Oehmigen, K., Hähnel, M., Brandenburg, R., Wilke, C., Weltmann, K. D., & Von Woedtke, T. (2010). The role of acidification for antimicrobial activity of atmospheric pressure plasma in liquids. *Plasma Processes and Polymers*, *7*(3-4), 250-257.

[128] Kawasaki, T., Eto, W., Hamada, M., Wakabayashi, Y., Abe, Y., & Kihara, K. (2015). Detection of reactive oxygen species supplied into the water bottom by atmospheric non-thermal plasma jet using iodine-starch reaction. *Japanese Journal of Applied Physics*, *54*(8), 086201.

[129] Uchida, G., Nakajima, A., Ito, T., Takenaka, K., Kawasaki, T., Koga, K., Shiratani, M., & Setsuhara, Y. (2016). Effects of nonthermal plasma jet irradiation on the selective production of H_2O_2 and NO_2^- in liquid water. *Journal of Applied Physics, 120*(20), 203302.

[130] Laroussi, M., & Leipold, F. (2004). Evaluation of the roles of reactive species, heat, and UV radiation in the inactivation of bacterial cells by air plasmas at atmospheric pressure. *International Journal of Mass Spectrometry, 233*(1-3), 81–86.

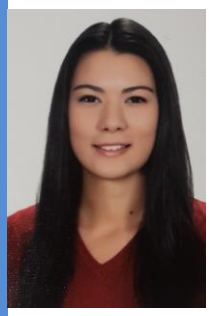

4 Şubat 1992

Bayraklı / İZMİR

+90 533 483 90 30

elifcukur@gmail.com

Elif ÇUKUR

CV

Eğitim Durumu

2006 – 2010 Gümüşpala Anadolu Lisesi (İzmir)

2011 – 2015 Erciyes Üniversitesi (Kayseri)

Mühendislik Fakültesi, Biyomedikal Mühendisliği

2014 – 2015 Lublin University of Technology (Poland / Lublin)

Electrical Engineering and Computer Science

2016 – 2019 İzmir Katip Çelebi Üniversitesi (İzmir)

Fen Bilimleri Enstitüsü, Biyomedikal Teknolojiler A.B.D.

Tezli Yüksek Lisans

Staj

2013 Dokuz Eylül Üniversitesi Eğitim ve Araştırma Hastanesi (İzmir)

(Klinik Mühendisliği Departmanı)

2014 EvoluCare Tıbbi Yazılım ve Donanım Ltd. Şirketi (İstanbul)

Sertifikalar

2012 TMMOB Elektrik Mühendisleri Odası Ankara Şubesi

- Biyomedikal Mühendisliği, Girişimcilik ve İnovasyon
- Tıbbi Alanlarda Topraklama

2015 Tüm Radyoloji Teknisyenleri ve Teknikerleri Derneği (TÜMRAD-DER)

22. Uluslararası Tüyap ExpoMED Sağlık Fuarı

- Dünden Bugüne Radyoloji Semineri

2015 TOBB Ekonomi ve Teknoloji Üniversitesi

Sağlık ve Biyomedikal Bilimler Topluluğu

- Future Medicine'15

2017 TıpTekno'17, Tıp teknolojileri Kongresi

Yayınlar

- Çukur, E., Yıldırım, Ç., Ercan, U. K., Degradation of Tattoo Inks by Non-Thermal Atmospheric DBD Plasma Treatment for Plasma Assisted Tattoo Removal Purpose. 7th Central European Symposium on Plasma Chemistry (CESPC 7), September 3-7, 2017, Sveti Martin na Muri, Croatia (Poster Sunumu).
- Elif Çukur, Utku Kürşat Ercan, Soğuk Atmosferik Plazma (SAP) Kullanarak Dövme Silme. Tıp Teknolojileri Kongresi, 12-14 Ekim 2017, Trabzon, Türkiye (Sözlü Bildiri).
- Çukur, E., Yıldırım, Ç., Ercan, U. K., Degradation of Tattoo Inks by Cold Plasma. 7th International Conference on Plasma Medicine (ICPM 7), June 17-22, 2018, Philapelphia, USA (Poster Sunumu).
- Ercan, U. K., İbiş, F., Dikyol, C., Horzum, N., Karaman, O., Yıldırım, Ç., Çukur, E., Demirci, E. A., 2018, Prevention of Bacterial Colonization on Nonthermal Atmospheric Plasma Treated Surgical Sutures for Control and Prevention of Surgical Site Infections. PLoS ONE 13 (9): e0202703.
- Gökçelli, U., Ercan, U. K., İlhan, E., Argon, A., Çukur, E., Üreyen, O., 2018, Prevention of Peritoneal Adhesions by Non-Thermal Atmospheric Plasma Treatment on Mouse Model. British Journal of Surgery-1301-Aug-18.

Bilgisayar Bilgisi

AutoCAD, C Programlama Dili, C# Programlama Dili, MATLAB, Simulink, LabView.

Katıldığı Sınavlar

ALES 2014 - SAY	79,43
ALES 2015 - SAY	77,77
YDS 2016	76,25
YÖKDİL 2017	75,00

Dil Yeteneği

İngilizce (Okuma: İleri düzey, Yazma: İyi düzeyde, Konuşma: İyi düzeyde)